UCRL-10701

University of California

Ernest O. Lawrence Radiation Laboratory

PREDICTION OF HIGH TEMPERATURE METALLIC PHASE DIAGRAMS

Berkeley, California

UCRL-10701
UC-25 Metals,
Ceramics and
Materials

UNIVERSITY OF CALIFORNIA
Lawrence Radiation Laboratory
Berkeley, California

Contract No. W-7405-eng-48

PREDICTION OF HIGH TEMPERATURE METALLIC PHASE DIAGRAMS

Leo Brewer

July 1963

UCRL-10701

PREDICTION OF HIGH TEMPERATURE METALLIC PHASE DIAGRAMS

Leo Brewer

Inorganic Materials Research Division
Lawrence Radiation Laboratory
and Department of Chemistry
University of California
Berkeley, California

Abstract

The Engel correlation between electronic configurations and crystal structures of metallic phases is confirmed and applied to the binary and multicomponent systems of the thirty metals of the three transition series from the alkali metals to the nickel-platinum group. The use of the Engel correlation to obtain electron configurations and the application of internal pressures of the metals to the regular solution theory together with consideration of the sizes of metal atoms makes possible the prediction of unknown phase diagrams. Diagrams are given as projections upon a composition scale and composition ranges given are the maximum extent over the entire temperature range of the solid phases.

Of the two billion possible multicomponent phase diagrams of the thirty metals, at least one and a half billion are readily obtained from the figures, tables, and text and methods are described for extending the procedures for prediction of phase diagrams to additional diagrams outside the range of metals considered.

I. Introduction

The knowledge of high temperature phase diagrams is important for the design of high temperature purification processes such as zone refining, vaporization of materials away from impurities, vaporization of impurities by vacuum heating, and other purification processes. Such processes can be expected to play an important role in the production of semiconductors, superconductors, and other materials requiring high purity. There is evidence that certain structures are particularly favorable for high critical superconducting temperatures and fields and phase diagram information is needed to indicate the composition ranges that can be prepared with a given structure.

The present paper deals with the predictions of the multicomponent phase diagrams for the thirty metals of the three transition series from potassium through nickel, rubidium through palladium, and cesium through platinum. The complete description of the phase behavior of these metals in various combinations requires over two billion diagrams. For example, there are 582,000,000 fourteen-component diagrams, 142,500 four-component diagrams, and even 435 diagrams are required for only the binary systems. It is clear that it is not possible to establish so many diagrams experimentally in the forseeable future and one must correlate theory with existing data to predict the missing information.

II. CONFIRMATION OF ENGEL CORRELATION

In this paper the Engel[1,2] correlation between electronic configuration and crystal structure is used together with the regular solution theory[3,4,113] of solubilities to predict the structures of the various phases of a diagram and their ranges of composition. The Engel model ascribes the occurrence of the body-centered cubic structure (Structure I), the hexagonal close-packed structure (Structure II), and the face-centered cubic structure (Structure III) to concentrations of one, two, and three valence electrons per atom, respectively, with these valence electrons in the s or p state. Electrons in d states are not supposed to influence the crystal structure. The Engel model provides the opportunity to make rather straightforward correlations to determine the distribution of electrons between d states on one hand and s or p states on the other hand and therefore to predict the crystal structure as fixed by the average number of s or p electrons per atom. It has been shown previously[1,2] that the Engel bonding model does yield a satisfactory correlation with existing data. However, it is of value to provide an independent confirmation of the Engel correlation.

Moore[5] has compiled the existing data on the known electronic states of the gaseous atomic elements. The spectroscopic state designations are listed together with the excitation energies of the states and the electron configurations corresponding to each state. As an example, the ground electronic state of potassium is listed as a ^2S state corresponding to an electron configuration beyond the closed shells of a single s electron. The first excited state is a

^2P state with an excitation energy of 37 kcals/mole and corresponds to a single p electron. The ^2D state corresponding to a single d electron has an energy of 62 kcal/mole above the ground ^2S state and a promotion energy of 62 kcals/mole is required to promote the s electron of the ground state of potassium to a d electron. All of these configurations provide one electron per atom for bonding.

The data tabulated by Moore can be used to determine the promotion energy required to obtain the various electronic configurations corresponding to the specific crystal structures indicated by Engel's correlation. Two electronic configurations with the same number of unpaired electrons available for bonding, e.g. d^5s and d^4sp, would be expected to yield comparable bonding energies. Thus if one configuration requires a much higher promotion energy than another, the crystal structure corresponding to the configuration of higher energy would be predicted to be unstable.

The procedure can be illustrated by the data of Table 1 for the sixth group elements Cr, Mo, and W. The first three columns of numbers are the promotion energies of the ^7S, ^5D, and ^7F states which are the lowest electronic states corresponding to the electronic configurations d^5s, d^4s^2, and d^4sp, respectively[6]. The promotion energies show that a hexagonal close-packed Structure II corresponding to the d^4sp electronic configuration would be quite unstable compared to the body-centered cubic Structure I corresponding to the d^5s configuration. The d^4s^2 configuration is of no value for the metallic state as the paired s electrons are not available for bonding and this configuration would yield only four bonding electrons per atom

compared to the six bonding electrons per atom of the other two configurations. No data are available for the d^3sp^2 configuration but all indications point to a very high promotion energy which would make the face-centered cubic Structure III unstable. The fifth column tabulates the enthalpy in kcal/mole liberated when gaseous atoms in the $^7S(d^5s)$ state are condensed to the metallic state. These values are obtained by adding the promotion energy, if any, to the enthalpy of sublimation. For the present purposes, it is sufficiently accurate to combine the enthalpies of sublimation at 298°K tabulated by Brewer[2,114] with the promotion energies at 0°K tabulated by Moore[5]. The hexagonal close-packed Structure II would be stable for Cr, Mo, and W, if the six bonding electrons of the d^4sp configuration yielded bonding energies of 165, 238, and 255 kcal/mole respectively. These are much larger than the energies of 95, 158, and 209 kcal/mole obtained by using the six electrons of the d^5s configuration for bonding between atoms in the metal. There is no reason to expect that the six bonding electrons of one type would yield very greatly different bonding energies than the six bonding electrons of the other type. Thus we have an excellent independent confirmation of the Engel theory as the spectroscopic data for the gaseous atom rule out any electronic configuration for the metal other than the configuration with a single s electron corresponding to the observed body-centered cubic structure.[2,14,115]

In Table 2, similar data are presented for the fifth group elements V, Nb, Ta. Although the differences are smaller, the d^4s configuration with five bonding electrons is clearly the only stable configuration to be expected for V and Nb. Within the uncertainty of using energies

of lowest electronic levels corresponding to an electronic configuration[6], one can not completely rule out Structure II for Ta, particularily under high pressure, but the Structure I has an advantage of around 22 kcal/mole.

From the occurrence[2,115] of the body-centered cubic Structure I for the Fifth and Sixth Group transition metals, Engel's rule predicts d^4s and d^5s electronic configurations, respectively. The above discussion shows that the spectroscopic data confirm Engel's prediction.

Table 3 shows the data for the Fourth Group metals. The configurations d^3s and d^2sp with four unpaired electrons available for bonding are close enough in energy, within the accuracy of our procedure of using the energies of the lowest electronic states of each configuration, so that the occurrence[2,115] of both structures I and II is consistent with the spectroscopic data. The last two columns list the bonding energies obtained by adding the promotion energies to the enthalpy of sublimation[2,114] at 298°K. The differences in enthalpy of sublimation of the two structures is ignored. If average promotion energies of the electron configuration are used[6], the promotion energies are closer and the two bonding energies are brought closer together, but the d^2sp configuration still has a slightly higher bonding energy than the d^3s configuration.

In Table 4, the comparison of the promotion energies for the various electronic configurations of Al with those of Sc, Y, and La is particularily instructive. For Al, the two lowest configurations s^2p and s^2d are not of value for the metal because the paired s electrons are not available for bonding and one s electron must be promoted to a p or d state to make three electrons available for bonding. No data are available for the d^2s configuration for Al, but all indications are

Table 1. Promotion Energies and Bonding Energy for Sixth Group Metals, kcal/mole.

	$d^5s(^7S)$	$d^4s^2(^5D)$	$d^4sp(^7F)$	d^5s bond	ΔH_{subl}
Cr	0	23	70	95	95
Mo	0	31	80	158	158
W	9	0	55	209	200

Table 2. Promotion Energies and Bonding Energy for Fifth Group Metals, kcal/mole.

	$d^3s^2(^4F)$	$d^4s(^6D)$	$d^3sp(^6G)$	d^4s bond	ΔH_{subl}
V	0	6	47	129	123
Nb	0	3	47	176	173
Ta	0	28	50	215	187

Table 3. Promotion Energies and Bonding Energies for Fourth Group Metals, kcal/mole.

	$d^2s^2(^3F)$	$d^3s(^5F)$	$d^2sp(^5G)$	d^3s bond	d^2sp bond
Ti	0	19	45	132	158
Zr	0	14	42	160	188
Hf	0	40	51	200	211

Table 4. Promotion Energies of Third Group Metals, kcal/mole.

	$s^2p(^2P)$	$ds^2(^2D)$	$d^2s(^4F)$	$dsp(^4F)$	$sp^2(^4P)$
Al	0	92		190	83
Sc	97	0	33	45	
Y	30	0	31	43	
La	44	0	6	40	

that it has a very high promotion energy and that Structure I would be very unstable for Al. Structure II corresponding to the configuration d sp is seen to be unstable by over 100 kcal/mole. Thus Structure III corresponding to electronic configuration sp^2 is the only possible structure. In contrast, the electronic configuration of Sc, Y, and La with three bonding electrons that has the lowest promotion energy is d^2s corresponding to Structure I while the d sp configuration is not much higher in energy. For Sc, the number of levels to be averaged is small enough and sufficient data are available to allow the calculation of the average energies of the configurations[6]. Thus the average energies for d^2s and d sp are found to be 50 and 58 kcal/mole, respectively compared to 33 and 45 kcal/mole for the lowest electronic states of the configurations. The best available data[15,115] indicate that Sc, Y, and La all have the body-centered cubic Structure I at high temperatures and the hexagonal close-packed Structure II at lower temperatures in agreement with the expectations from the spectroscopic data and Engel's correlation. La also has the face-centered cubic Structure III, but no data are available to calculate the promotion energy of the sp^2 configuration of La. A high promotion energy is expected for this configuration. Since the bonding energies of the d sp configurations are slightly higher than for the d^2s configurations, the higher promotion energy of the sp^2 configuration might be offset to some extent by a high bonding energy, but one would not expect a substantial difference in bonding energy. In the absence of data for the promotion energy of the sp^2 configuration, one can not say whether the occurence of Structure III constitutes a contradiction to the

Engel correlation although one would not have predicted its occurence a priori.

Table 5 presents the promotion energies for the alkaline earth metals. The data[5] are complete enough and the calculation simple enough to allow tabulation of the average energy of each configuration rather than the energy of the lowest state of the configuration[6]. The data for Mg exclude any bonding configuration other than sp and therefore any structure other than Structure II. The sp and sd configurations for Ca, Sr, and Ba are close in energy. The body-centered cubic Structure I corresponding to configuration sd is found[2,14,115] at high temperature for Ca and Sr and at all temperatures for Ba. Sr also has Structure II. The non-occurrence of Structure II for Ba is consistent with the promotion energies. One would have expected Structure II for Ca, but pure Ca apparently does not show this structure[14]. Ca and Sr also have the face-centered cubic Structure III. Such a structure seems incompatible with the Engel correlation. It would require promotion of an electron from a closed shell to the configuration $p^5 d$ sp. Such a configuration should have a considerable promotion energy although no data are available, but it would have four bonding electrons which might yield enough extra bonding energy to make up for the additional promotion energy. One would not have predicted the occurrence of these structures a priori.

Examination of the bonding energies of the various electron configurations tabulated in Tables 1-5 together with the additional data to be presented show that generally the bonding energy of a d electron increases very markedly with nuclear charge from the first transition series to the third transition series. Thus the bonding

Table 5. Promotion Energies of Electron Configurations of Alkaline Earth Metals, kcal/mole.

	s^2	sp	sd
Mg	0	80	140
Ca	0	55	60
Sr	0	52	56
Ba	0	44	29

Table 6. Promotion Energies and Bonding Energy for Seventh Group Metals, kcal/mole.

	$d^5s^2(^6S)$	$d^6s(^6D)$	$d^5sp(^8P)$	d^5sp bond
Mn	0	49	53	120
Tc	0	6	46	202
Re	0	35	56	243

Table 7. Promotion Energies and Bonding Energy for Eighth Group Metals, kcal/mole.

	$d^6s^2(^5D)$	$d^7s(^5F)$	$d^6sp(^7D)$	d^6sp bond
Fe	0	22	57	< 157
Ru	19	0	70	223
Os	0	15	70	257

energy of the d^5s configuration is 114 kcal/mole larger for W than for Cr or 23 kcal larger per d electron. The data for the transition elements of the fourth to seventh groups, considering both structures I and II, show increased bonding energies for the third transition series compared to the first transition series ranging between 21 and 23 kcal per d electron. This trend is in contrast to the almost universal trend among all types of compounds[2] for bonds involving only s and p electrons to decrease in bonding energy as one moves downward in the periodic table to larger nuclear charge. The effect of increased nuclear charge upon the strength of d bonds must be due to contraction of the closed shells and increased exposure of the d orbitals relative to the closed shells to allow better overlap of d orbitals between atoms at the internuclear distances fixed by the balancing of attractive bonding forces by the repulsive forces due to interpenetration of the close shells.

It is of interest at this point to inquire why only the s and p and not the d electrons should influence crystal structure. In comparing the close-packed Structures II and III, the nearest neighbors are the same for two structures. Any differences have to do with more distant neighbors. The orbitals of the d electrons of an inner shell are much more contracted in space than the s and p orbitals of the outermost shell. One would expect bonding due to overlap of d orbitals to be restricted largely to nearest neighbors with little effect on long range order while bonding due to s and p electrons would be expected to range out into the metal for many atomic diameters. It is quite reasonable to accept Engel's hypothesis that d electrons do not influence crystal structure if extensive hydridization between the d

electrons on one hand and the s and p electrons on the other hand does not take place.

For the metals of the first six groups, electronic configurations with paired valence electrons were excluded as the promotion energies were smaller than the bonding energies and configurations that did not use all of the valence electrons for bonding were unstable in the metallic state. Beyond the first six groups, some configurations require pairing of some of the d electrons and not all configurations of importance will have the same number of bonding electrons. In addition to differences in promotion energies, one must consider differences in bonding energy due to different number of unpaired electrons. Table 6 shows the promotion energies for electronic configurations of the seventh group metals. Unfortunately no data are available for the d^4sp^2 configuration. The d^6s configurations with five bonding electrons have lower promotion energies than the d^5sp configurations with seven bonding electrons. Comparisons of bonding energies for other metals would indicate that the two extra bonding electrons for Tc and Re would contribute at least forty kcal/mole additional bonding energy which would make Structure II more stable than Structure I, in agreement with observation.[2,115] The bonding energies due to d^5sp bonds are 202 and 243 kcal/mole, respectively, for Tc and Re or 29 and 35 kcal per bonding electron. Thus, an electronic configuration with a high promotion energy can be the most stable configuration in the metal if it provides more bonding electrons than other configurations. For the metals of the second and third transition series which have large bonding energies due to more effective use of d electrons in bonding, the two additional bonding electrons provided by promotion of one d electron can offset a very large promotion energy. Table 7 shows a similar behavior for Ru and Os where the d^6sp configuration with six bonding electrons yields a more stable Structure II than the d^7s configuration of Structure I with only

four bonding electrons even though the additional promotion energy amounts to as much as 70 kcals. No data are available for the promotion energies of configurations of interest for Rh, Ir, Pd, Pt, Ag, and Au. All of these metals have the face-centered cubic Structure III corresponding to an sp^2 electronic configuration with from six to eight d electrons. The promotion energies required for the sp^2 configuration must be quite large. However, the promotion of d electrons to s and p states unpairs d electrons and makes them available for bonding.

Before turning to the behavior of the metals of the first transition series, it is instructive to examine the trend of bonding energy per bonding electron for the metals of the second and third transition series as one goes from left to right in the periodic table. The s bond of the alkali metals provides around 20 kcal bonding energy per electron. The sp and sd configurations of the alkaline earth metals yield bonding energies of 36-47 kcal per bonding electron. The d sp and d^2s configurations of the third group metals yield bonding energies of 40-50 kcal per bonding electron. The fourth group configurations d^2sp and d^3s yield over 50 kcal per bonding electron. In dealing with promotion energies and relative stabilities of structures, it was possible to ignore the difference between the energy of the lowest state of a configuration and the average energy of an electron configuration[6] because of similar corrections for the various configurations. This difference can not be neglected for absolute values of the bonding energies and the values cited above for the first fourth groups have been corrected approximately to the value corresponding to the average energy of the electronic configurations. The increase in effectiveness of a bonding electron in going from left to right in the periodic table reflects the effect of

increasing nuclear charge in shrinking the closed shells. This reduces the size of the closed shells, thus, allowing closer approach of the atoms and more effective overlap of electron orbitals. Beyond the d^3s configuration, there appears to be a reduction in effectiveness of a bonding electron as one approaches the d^5s configuration. Without going to the effort of calculating the average energies of the electron configurations,[6] the exact extent of this reduction is not clear. If one merely uses the energy of the lowest electronic state corresponding to a given configuration, the total bonding energies change from 160 to 176 to 158 kcal/mole for $Zr(d^3s, {}^5F)$ to $Nb(d^4s, {}^6D)$ to $Mo(d^5s, {}^7S)$ or a change in bonding energy per electron from 40 to 35 to 26 kcal. Likewise, for Hf to Ta to W, the bonding energy per electron changes from 50 to 43 to 35 kcal. The correction to the average energy of the electron configuration increases as one goes from d^3s to d^5s because of the increase in the total number of states corresponding to a given configuration. Thus, this correction will probably largely wipe out the apparent reduction in effectiveness of a bonding electron as one goes from the d^3s to d^5s configuration. However, there may be steric problems involved in using all five d orbitals in bonding that may reduce their effectiveness. The d^5sp configuration of Tc and Re yields bonding energies per bonding electron similar to those for the d^5s configuration. However, beyond Tc and Re, the bonding energies per bonding electron increase steadily. This is due in part to the decreasing number of electronic states for a given electronic configuration as the number of unpaired electrons decreases, which brings the energy of the lowest electronic state closer to the average energy of the configuration. A steric hindrance in the use of five d orbitals may also play a role, but the

effect must be due mostly to the effect of increasing nuclear charge in shrinking the closed shells and, thus, decreasing the repulsive contribution to the energy due to interpenetration of closed shells. This large contribution to the energy per bonding electron for the transition metals to the right of the periodic table, amounting to around 50 kcal per bonding electron, strongly favors the promotion of d electrons to increase the number of bonding electrons. Thus, the occurrence[115] of Structure III and electron configurations d^6sp^2, d^7sp^2, and d^8sp^3 for Rh and Ir, Pd and Pt, and Ag and Au, respectively, is in full agreement with the Engel correlation. Although no spectroscopic data are available for the sp^2 configuration, the data tabulated by Moore[5] indicate unusually high promotion energies to promote d electrons to the p state for Pd and Ag compared to Pt and Au. This is apparently the reason for the abnormally low net bonding energies and low sublimation enthalpies of Pd and Ag. The correspondingly low internal pressures or solubility parameters[3,4,113] then reduces the solubilities of Pd and Ag in the other transition metals.

The primary factor in the understanding of the behavior of the metals of the first transition series is the relative bonding ineffectiveness of the d electrons. It was noted previously that the bonding energies per d electron are over 20 kcal smaller for the first transition series than for the third transition series. Table 6 shows similar promotion energies for the d^6s and d^5sp configuration of Mn. One would expect Structure II with five bonding d electrons to be more stable than Structure I with only four bonding d electrons. It was noted above that there appears to be a reduction in the bonding stability of the d^5 configuration. Since d electrons do not bond strongly between atoms of

the first transition series, the actual stabilities of Structures I, II, and III are very close together for Mn. There are only a few other instances of metals with a number of electronic configurations yielding structures of comparable stability. U and Pu show similar behavior. The result is a structure like that of α-Mn, β-Mn, or the complex structures of U and Pu in which the same element can display different electronic configurations and, therefore, different radii and bonding characteristics in the same phase. Mn does form the simple Structures I and III, corresponding to d^6s and d^4sp^2. In the more complex structures, it undoubtedly takes on the configuration d^5sp in addition to the previous ones.

Table 7 shows that the promotion energy for the d^7s configuration of Fe is considerably smaller than the promotion energy of the d^6sp configuration. The relative ineffectiveness of the d bonding results in Structure I being more stable than Structure II. The magnetic behavior of Fe and the close-by metals of the first transition series is direct evidence that the d electron contribution to bonding is poor enough so that they are not used for bonding and are left unpaired. One does not observe this evidence of unpaired electrons for transition metals of the second and third series since the d electrons can be used so effectively in electron pair bonding , which removes their magnetic contribution. The occurrence of Structures II and III for Co and Structure III for Ni and Cu, which require promotion of paired d electrons to p states is probably to be attributed more to the effective use of additional p electrons in bonding than to the availability of additional unpaired d electrons.

III. PROCEDURE FOR APPLICATION OF ENGEL MODEL

The interpretation of the Engel correlation in terms of spectroscopic data for the gaseous atoms is not essential for the use of the Engel correlation in the prediction of metallic phase diagrams, but the confirmation shown above lends confidence to the use of the Engel theory in the following discussion.

The understanding of the phase behavior of the transition metals is complicated by the variety of factors that must be considered. A great deal of effort has been devoted to the evaluation of the important factors. The previous publications are too extensive to be reviewed here, but recent reviews[7-13, 40, 43, 44] cover the earlier papers. It is generally agreed that the primary factor which fixes the thermodynamic properties of metallic solutions is the electronic structure of the components. Important secondary factors, which are, in turn, functions of the electronic structure, are size, electronegativity, and internal pressure or solubility parameter. The present treatment follows previous efforts by setting up a model which incorporates the various factors and attempts to determine the variation of their influence in various alloys across the periodic table. Because of the number of variables, it is important to make their application as explicit as possible. Unless otherwise noted, all experimental data used in the following correlations are from Hansen and Anderko,[14] Lunden,[15] and Matthias, Geballe and Compton.[16]

The Engel correlation between crystal structure and electronic configuration allows one to fix the major variable. In the previous discussion, Structures I, II, and III have been assigned to the electronic configurations corresponding to one, two, and three electrons per atom, respectively, of the s or p type. Examination of the

composition ranges with body-centered cubic Structure I for non-transition metal alloys or metals of known valence indicates that Structure I actually is stable up to 1.5 electrons per atom of the s or p type. The hexagonal close-packed Structure II is found for the Hume-Rothery[17] phases $LiCd_3$, $CuZn_3$, Cu_3Sn, and $AgZn_3$ and for solutions of Li in Mg and Zn with electron to atom ratios as low as 1.7. On the other side, the electron to atom ratios are just slightly above two in the Ga-Mg and Al-Zn systems with a maximum value of 2.12 in the Al-Mg system. From these results, Structure II is seen to be restricted to s,p electron to atom ratios of 1.7 to 2.1. The solid solubilities of Li, Mg, and Zn in face-centered cubic Al indicate that the electron concentration may drop to below 2.5 electrons per atom and still retain Structure III, but the solid solubilities of Si and Ge in Al indicate that the concentration cannot rise appreciably above three.

The fundamental assumption of Engel's model is that the d electrons do not directly fix the crystal structure. With the assignment of ranges of s,p electron concentrations to each structure, the knowledge of the structure fixes the s,p electron concentration within the indicated ranges and therefore fixes the concentration of d electrons in transition metal systems by difference.

Engel, in agreement with others,[18] expects the unfilled d shells of the first half of the transition elements to act as sinks for electrons and, thus, to tend to keep the concentrations of s or p electrons below the 1.7 lower limit of Structure II. In the previous discussion, it was seen that the promotion energies required to promote d electrons to p electrons were sufficient to favor the body-centered cubic Structure I. In agreement with this, all of the transition metals of the

first six groups have[2,14,15,115] Structure I at least at high temperatures, if not at all temperatures. The elements of the earlier groups cannot trap electrons as strongly in the d shell as those of the later groups, and Sr and the third and fourth group metals transform upon cooling to Structure II. The change in electronic structure on the basis of the Engel model is from $d^{1.5}s^{1}p^{0.5}$ for body-centered cubic Y, for example, to $d^{1.3}s^{1}p^{0.7}$ for hexagonal Y. The recognition that the various structures are not restricted to integral electron concentrations requires some modification of the previous discussion which was restricted to integral concentrations. Thus, Mo and W, for example, would be expected to dissolve up to a maximum of 50 atomic % Tc or Re, corresponding to an average electronic configuration $d^{5}s^{1}p^{0.5}$, and still retain the body-centered cubic Structure I. Reference to the phase diagrams to be presented in Section VIII below shows that the maximum solubilities range from 37 to 45 atomic %.

As another illustration, the system Mo-Pt can be considered. To attain the limiting configuration $d^{5}s^{1}p^{0.5}$, 12 atomic percent Pt would have to dissolve in Mo with Structure I. Addition of more Pt should cause a transformation to Structure II which would be predicted to lie between 18 and 28 atomic percent Pt corresponding to the range in electronic configuration from $d^{5}s^{1}p^{0.7}$ to $d^{5}s^{1}p^{1.1}$. Finally, one would predict the face-centered cubic Structure III between 38 and 100 atomic percent Pt corresponding to the range $d^{5}s^{1}p^{1.5}$ to $d^{7}s^{1}p^{2}$. Actually, from the behavior of Pt in other alloy systems, it is found that it is very difficult to reduce the d concentration in Pt all the way to the d^{5} configuration, particularly when the other metal is not of the third transition series. The procedure in the use of Engel's model is to translate all of the known structural data into electronic configurations which give the respective concentrations of d and of s,p electrons. This, then

provides information of the variation in the stability of the d configuration across the periodic table. With alloy systems involving elements in the middle of the second and third transitions series, one finds that the metals tend to the d^5 configuration with a minimum promotion of d electrons to the p state. For metals of the early groups, it is more difficult to build up the d configuration as high as d^5 and for later groups it is more difficult to drain off d electrons to a configuration as low as d^5. Examination of the available data allows one to predict the extent to which these early and late group metals will deviate from the d^5 configuration. Returning to the Mo-Pt system, Pt would be expected to assume a d^5 configuration only in the Mo rich region of Structure I, would be expected to have a configuration between $d^{5.5}$ and d^6 in the hexagonal Structure II region, and a configuration between d^6 and d^7 in the Structure III region.

The fixing of accurate limits of each region depends upon factors other than electron concentration. The limits of stability of a phase do not depend alone upon properties of the phase in question, but are also fixed by the properties of the saturating phases. If a phase diagram containing several intermediate phases is studied under conditions where the saturating phase can be changed through proper seeding, for example, with other conditions the same, then the solubility limits of the phase are changed. For this problem, one must consider factors such as atomic sizes and solubility parameters.[3,4,113] For the range of metals to be considered here, differences in electronegativity need not be considered separately as this factor is included in the use of the Engel correlation to fix variation of electronic configurations. For the Mo-Pt system even size and solubility parameters differences are

small, and the effect of these factors will be illustrated for other systems. The final predictions for the Mo-Pt system in atomic percent are as follows: Structure I, 0-12% Pt; Structure II, 30-53% Pt; Structure III, 63-100% Pt. These values represent the maximum ranges expected in the complete phase diagram. At lower temperatures, the ranges will decrease and ordering phenomena may arise which can result in miscibility gaps within each structure region.

Although the limits of each region depend upon the adjoining saturating phase, it is convenient to consider each structure separately. The structures to be considered are the I, II, and III structures already discussed. In addition, there are the Cr_3Si, σ, and α-Mn structures[12,40,43,44] which are found for s,p electron concentrations between 1 and 2 electrons per atom when proper size ratios are satisfied and, finally, the Laves phases and similar phases which depend very strongly upon size factors[44,45] although electronic configuration still plays a role.[12,13,19,20,43,44]

The elements of the first transition series require different treatment than those of the following series because of their poor utilization of d electrons in bonding. This makes the availability of unpaired d electrons more of an asset for stability for elements of the second and third series than for elements of the first transition series. The tendency of metals of the earlier groups to trap electrons in the d shells is reduced for the first transition series and metals of the later groups do not gain as much by promoting d electrons to make more d electrons available for bonding. Thus, in contrast to Tc and Re, which have only the d^5sp configuration corresponding to Structure II, Mn has both Structures I and III corresponding to configurations

$d^{5.5}s^{1}p^{0.5}$ and $d^{4.5}s^{1}p^{1.5}$ as well as complex structures in which the Mn atoms in different positions have different electronic configurations.

The flexibility of the transition elements with respect to electronic configuration is well established for their compounds for which a variety of oxidation states are found. The same is to be expected in metallic alloy systems. Just as gold may have oxidation states of one, two, and three in its compounds with non-metlas, similar variations are to be expected in its alloys and it has a valence of one when dissolved in non-transition metals[2] such as Al, Sn, etc., where no unpaired d electrons are available for bonding. It has a valence of three when dissolved in transition metals such as Ir and Pt which provide an environment of d electrons available for bonding and thus stabilize an electronic configuration for Au involving promotion of d electrons to p electrons. By use of the Engel correlation as a unifying concept to classify the trend in behavior of a given metal as its metallic environment is changed, it is possible to make reliable predictions of the behavior of transition metal systems. This procedure is illustrated below for each specific structure.

IV. OCCURRENCE OF THE BODY-CENTERED CUBIC STRUCTURE I AND THE LAVES PHASES

The previous discussion has shown that the considerable promotion energies required to promote d electrons to p states causes the body-centered cubic Structure I to be favored for metals of the first six groups. Crystal structure data[2,14,115] for the metals together with recent data for the rare earth metals[15] confirm that all eighteen metals of the first six groups of the three transition series have Structure I at high temperatures. Mixing of these metals does not affect the number of s,p electrons and can be considered merely as a mixing of d electrons. The absence of changes in s,p electronic configuration upon mixing allows simple application of the regular solution theory[3,4,113] to predict the mutual solubilities.

Application of the regular solution theory requires knowledge of the enthalpies of sublimation of the elements and their molal volumes. Accurate calculations would require values of the solubility parameter, $(\Delta E/V)^{1/2}$, for the metals at a variety of temperatures as tabulated by Hildebrand and Scott[3]. However, the regular solution theory is not expected to be accurate for solid solutions because there are other factors influencing solubility such as matching of sizes, etc. For the present purposes, it is quite adequate to use room temperature enthalpies of sublimation and volumes for calculations at all temperatures.[113] Errors due to this approximation as well as to neglect of other factors are most simply corrected by comparison of the deviations between available experimental data and predictions of the calculations carried out in the simplest manner possible. The enthalpies of sublimation used in the calculations for this paper are those given

by Brewer.[2,114] The molal volumes are calculated from the densities given by Hansen and Anderko[14] for the solid metal at room temperature. The equation[3,22]

$$T_c = (V/2R)\left[(\Delta E_1/V_1)^{1/2} - (\Delta E_2/V_2)^{1/2}\right]^2$$

with solubility parameters $\left(\frac{\Delta E_1}{V_1}\right)^{1/2}$ and $\left(\frac{\Delta E_2}{V_2}\right)^{1/2}$ yields the critical mixing temperature of metals 1 and 2 if their molal volumes do not differ much. Corresponding equations[3,22] allow calculations of the solubilities in one another below the critical temperatures.

The first step in the calculations is to calculate the solubilities of the various metals of a given group in one another, e.g., the solubilities of K, Rb, and Cs in one another. The calculations indicate that the liquids as well as the solids at temperatures near the melting point are miscible for metals of the same group. This prediction is in agreement with the known facts[14,15] for the first six groups. The highest critical temperature corresponding to the largest difference in solubility parameters is that for the Cr-W pair for which the simple regular solution calculation predicts a critical mixing temperature of 1600°K compared to the observed[14] critical temperature of 1768°K.

The next set of calculations deals with the solubilities of elements from different families in one another. The data are incomplete, but one can compare the available data with the predictions of the regular solution equation to give one an idea of what deviations from the predictions might be anticipated. In general, the liquids are more miscible than would be predicted from the regular solution equation using the enthalpies of sublimation and molal volumes of the solids at room

temperature due to smaller heats of vaporization and larger molal volumes for the liquids. For the solid phases, one finds in the majority of instances that the solid solubility is smaller than predicted by the regular solution equation, particularly when the sizes of the atoms are appreciably different. Thus, for example, for the pairs Cr-Ta, Zr-V, and Zr-Ta, (are miscible) the actual critical temperatures are two to three times higher than the calculated temperatures and complete miscibility of the solid phases is not observed even though the simple regular solution calculations would have indicated miscibility. Thus Zr and V are not misible with one another although their solubility parameters are close enough together to predict miscibility. The difference in solubility parameters of Zr and Nb is greater although miscibility is still predicted by the regular solution equation and in this instance the observations agree with the predictions of the equation. It is obvious that substantial differences in size will introduce strains in the solid lattice that will cause the activity coefficients to be higher than calculated by the regular solution equation. Although this is the usual direction of the deviation from the prediction of the regular solution equation for solid solubilities, the exceptions of the Ti-Ta and Ti-W systems might be noted for which the regular solution equation predicts small solubilities of the solid phases in one another at temperatures of the order of the melting point of Ti. The actual critical temperature is found to be substantially lower and large solubility is observed. Fortunately the range of solubility parameters of the metals is so large that one can make useful predictions to fix the order magnitude of phase behavior even with deviations of the type illustrated by the two Ti systems.

The high temperature phase behavior of the eighteen metals under consideration here can be summarized as follows. The alkali metals, K, Rb, and Cs with solubility parameters, $\left(\frac{\Delta E}{V}\right)^{1/2}$, of 22, 19, and 16 $(cal/cc)^{1/2}$, respectively, have mutually miscible liquid phases and also miscible solid phases at temperatures in the vicinity of the melting point. The solubility parameters of these alkali metals are so much lower than those for any of the other metals being considered here that one can confidently predict negligible solubilities in the solid phases of the other 15 metals. Even the liquid phases will be immiscible although the pair K-Ba would be expected to show considerably liquid solubility in one another near the boiling point of potassium.

Liquid Ca, Sr, and Ba with solubility parameters 40, 34, and 34 $(cal/cc)^{1/2}$, respectively, are expected to be mutually miscible. Below the melting point the body-centered cubic phases of these alkaline earth metals are expected to be mutually miscible also. The solubility parameters of these three alkaline earth metals differ sufficiently from the solubility parameters of the other metals being considered here, that one would predict that the solubilities in the solid phases of any of the other metals being considered would be very small. Even the liquids would not be miscible with the liquids of the other metals although substantial metal solubilities of Ca and La liquids would be expected at the boiling point of calcium in addition to K-Ba pair mentioned above.

The metals Sc, Y, and La with solubility parameters 76, 70, and 67, respectively, would be expected to be miscible in the liquid state and to have mutually miscible body-centered cubic solid phases below the melting point. Combinations of these third group metals with metals of

the other groups would be expected to show miscibility of the body-centered cubic phases only for the pairs Sc-Ti and Sc-Zr. For the next most soluble pair, Y-Ti, a predicted critical temperature of 2400°K for the solid phases agrees very closely with the experimental observation.[15] Sc and Y liquids should be miscible with Ti, Zr, and Hf liquids at high temperatures, but immiscibility is to be expected even for the liquid phases with metals of the fifth and sixth groups except possibly for Sc-V and Sc-Cr. Lanthanum with its very low solubility parameter would be expected to have liquid phase immiscible with even the fourth group metals liquids.

The solubility parameters of the transition metals of the fourth, fifth and sixth groups are in the range 103-131 except for 146 $(\text{cal/cc})^{1/2}$ for W and, considering the higher melting points, are close enough together so that all pairs of liquids should be miscible and considerable solid solubility can be expected near the melting points. Many of the diagrams are known[14] and confirm the regular solution predictions of solid miscibility for metals of the same group. Solid Nb which has an intermediate solubility parameter is miscible with all the transition metals of the fourth, fifth, and sixth groups. Similarly solid Mo is miscible with all except Zr and Hf. Solid W with the highest solubility parameter is miscible only with solid Mo, Cr, Ta, and Nb although V-W should be close to solid miscibility. Solid Ta behaves generally the same as W except for higher solid solubilities. Ti is miscible with Ta although Cr is not. Ti with the lowest solubility parameter of the nine metals is abnormally soluble since it is reported to be miscible with all but W. Zr shows lower solubilities than might be expected from its solubility

parameter in that it is reported to be miscible in the solid state with only Nb in addition to Ti and Hf. Some of the reported data may be in error due to non-metallic inpurities. Hf is expected to behave similarly to Zr but with larger solid solubilities. Since solubilities are usually larger than the regular solution predictions for pairs of metals of the same transition series, the Hf-Ta system may achieve miscibility near the melting points. Thus a rather complete picture can be given of the composition ranges of the body-centered cubic phases of the eighteen metals of the first six groups.

Up to this point no solid phases other than the body-centered cubic phase have been considered. In the binary systems a transformation can take place upon cooling with formation of a Laves phase.[12,13,44,45] These are phases with ideal compositions AB_2 and AB_5 and can occur in one of five closely related structures: the hexagonal $MgZn_2$, $MgNi_2$, and $CaCu_5$ structures and the cubic $MgCu_2$ and UNi_5 structures. In addition to the compositions AB_2 and AB_5, Laves phases with intermediate structures are found[21,100] at compositions AB_3, A_2B_7, and AB_4 and defect AB_5 structures occur up to the composition AB_6. In some of the binary systems of the actinides and lanthanides with nickel and copper, a series of such Laves phases occur between the composition AB_2 and AB_6. Electronic configurations determine which of the structures forms,[12,13,19,44] but the ratio of the radii of A and B is the primary factor in determining whether a Laves phase will form and all of the Laves structures will be considered together in the present discussion. Dwight[13] and Nevitt[44] have discussed in detail the various factors which determine the occurrence of Laves phases. In these phases, a closer packing is achieved than is possible with close packing of equal size spheres and the A atom

is coordinated in AB_2 by 12 B plus 4 A atoms. The optimum packing occurs when the size of the A atom is 23% greater than the size of the B atom.

In the AB_5 structures, all A-A contacts are replaced by A-B contacts and the optimum packing occurs when the size of the A atom is 30 to 45% greater than the size of the B atom.[44] As the size of the metallic atoms decrease steadily from left to right in the periodic table, the Laves phases contain B atoms which are to the right of the A atoms in the periodic table or which are considerably higher in the periodic table to insure that the B atom is sufficiently smaller than the A atom. In addition, the solubility parameters can not be too greatly different. K, Br, and Cs are not reported to form Laves phases with the B conponent any metal to the left of the Cu-Au group although Mn has a low enough solubility parameter to allow formation of a Laves phases. It would be interesting to investigate mixtures of Mn with Li or Na or to reduce Mn compounds by solutions of alkali metals in liquid ammonia to determine if a Laves phase could be prepared. Ca, Sr, and Ba are not known to form any Laves phases with transition metals to the left of the ninth group but $CaNi_5$ and MPt_5 are known[21] and AB_2 phases are known with Rh, Pd, Ir, and Pt.[44] Ca, Sr, and Ba also form AB_2 phases with the smaller Mg. The third group transition metals and the lanthanides and actinides form AB_2 and AB_5 phases with transition metals to the right of the sixth group.[44] None of the Laves phases mentioned so far have had any occurrence in phase diagrams among the first six groups of the three transition series. However, Zr and Hf have sufficiently large solubility parameters that Laves phases can be formed with any of the metals with radii sufficiently smaller than the radii of Hf or Zr. Thus AB_2 phases are known or can be expected for Zr and Hf with V and all of the transition metals of the sixth, seventh, eighth, and ninth groups. Zr and Hf form phases with Ni and

probably Co of the UNi_5 type over a range of compositions. The smaller Ti, on the other hand, forms Laves phases only with the first transition series metals Cr, Mn, Fe, and Co. The radius ratios of the components of a Laves phase are different from the ratios for the pure metals since charge transfer or electron transfer undoubtedly takes place between elements of different electronic configuration and the resulting radii will be those corresponding to ions of the intermediate charge. However, for closely adjacent elements of similar electronegativity the use of the metallic radii of the pure elements is a useful guide in predicting the occurrence of Laves phases. Nb and Ta are too small to form Laves AB_2 phases with metals of the second and third transition series, but they can form Laves phases with Cr, Mn, Fe and Co.

In the phase diagrams among the metals of the first six groups under discussion, the Laves phases decompose peritectically with the exception of $ZrCr_2$ and $HfCr_2$ which melt congruently and the occurrence of the Laves phases does not influence the phase behavior in the vicinity of the liquidus and solidus curves. However, the occurrence of the Laves phase in the Cr-Nb, and Cr-Ta systems is undoubtedly responsible for the smaller solid solubilities due to reduced activities of the elements than would be expected from the regular solution equation. Only in the Cr-Zr and Cr-Hf systems does the occurrence of the Laves phase make a substantial difference in the high temperature behavior in the vicinity of the liquidus curves. The type of interaction responsible for the Laves phase must also persist in the liquid phase causing a depression of the liquidus curves compared to ideal solution behavior. This results in poor distribution

coefficients between the solid and liquid phases for the zone refining process. Although the other Laves phases do not influence high temperature behavior in the vicinity of liquidus curves, they are, of course, of interest as low temperature phases of unusual properties.

The only other intermediate phase that occurs in the phase diagrams among the elements of the first six groups is a samarium type structure which is found in binary diagrams of the various third group transition metals and the rare earth metals. This structure is not of high stability and does not affect the solidus and liquidus curves.

In the discussion of phase diagrams involving the first six groups of the periodic table, the problem of relationship between crystal structure and electronic structure is very simple since all of the metals have the body-centered crystal structure at high temperatures, which is to be attributed to the stabilization of the electron structure with a minimum number of electrons in the s and p states and the remainder in the the d state. For transition elements to the right of the sixth group, the body-centered cubic structure with only one s or p electron per atom cannot be maintained unless d electrons are paired and thus made unavailable for bonding. In the previous discussion it was noted that metals of the first transition series such as Cr, Mn, Fe, and Co do not utilize d electrons efficiently in bonding. This results first in the lack of pairing of d electrons between the atoms, which occurs when bonding takes place, and thus ferromagnetic behavior due to the retention of unpaired d electrons. Secondly this results in the appearance of the body-centered cubic structure for manganese and iron. On the other hand, the heavier

transition elements gain sufficient energy through use of unpaired d electrons in bonding so that the seventh group elements, Tc and Re, have only the hexagonal close-packed structure. To complete our discussion of the occurrence of Structure I, it is necessary to consider the extent to which metals of groups 7 to 10 can be dissolved in body-centered cubic metals before a transformation takes place to Structure II or other structures.

It is fortunate the Hume-Rothery and his associates[23-26,43,101] have carried out systematic phase diagram studies for Fe and Mn rich compositions and have made accurate measurements of the solubility limits of each of the structures. All available data for the maximum concentrations of added transition metal in atomic percent are given in Table 8 for body-centered cubic Mn. The ranges around 50% given for Rh, Pd, Ir, and Pt correspond to the ordered body-centered cubic CsCl phases which will be discussed in more detail below. In Table 9, solubility limits are given for the body-centered cubic phase of Fe. The data given in these tables were obtained from Hellawell and Hume-Rothery,[23] Gibson and Hume-Rothery,[24] Hellawell,[25] and Hume-Rothery[26] together with earlier data from Hansen and Anderko.[14] In addition Savitskii and Kopetskii[27,28,29] presented additional data on the Ti-Mn and Zr-Mn systems, the Nb-Mn system, and the Ta-Mn system. Savitskii, Tylkina, Kirelenko, and Kopetskii[30] give the Re-Mn diagram. The values in parentheses are estimated values for systems for which no experimental data are available.

The trends in both tables are generally consistent with the Engel correlation and the solubility parameter differences. The effect of electron configuration of the added metal is best seen with minimum complication

Table 8. Maximum Concentrations in Body-Centered Cubic(I) Manganese in Atomic Percent.

Sc	Ti	V	Cr	Mn	Fe	Co	Ni	Cu
1	7.5	100	14	100	12	9	5.5	12.5
Y	Zr	Nb	Mo	Tc	Ru	Rh	Pd	Ag
0.5	1.5	2.4	(4)	(5)	8	4,33-55	3.9,38-68	1.5
La	Hf	Ta	W	Re	Os	Ir	Pt	Au
(0.4)	(0.8)	(1)	(2)	5	(4)	3,36-51	2,33-60	2,31-67

Table 9. Maximum Concentrations in Body-Centered Cubic(I) Iron in Atomic Percent.

Sc	Ti	V	Cr	Mn	Fe	Co	Ni	Cu
(1)	9.8,50	100	100	9.6	100	75	8	6.7
Y	Zr	Nb	Mo	Tc	Ru	Rh	Pd	Ag
(1)	5	3.8	26	(20)	5.5	2.9,50	3.3	< 0.2
La	Hf	Ta	W	Re	Os	Ir	Pt	Au
(1)	(3)	2.3	13	~15	(5)	~20	~20	4

from internal pressure differences by comparing the solubilities in the body-centered cubic Structure I of Mn and Fe given in Tables 8 and 9 with the corresponding solubilities in the face-centered cubic Structure III of Mn and Fe given in Tables 14 and 15.

In the earlier discussion it was seen that the metals of the first six groups must suffer considerable promotion energies to attain a sp^2 configuration with no gain in the number of bonding electrons. Addition of any of these metals to Structure III of Mn and Fe would result in a reduction of the number of s,p electrons below the critical value of 2.5 and would thus decrease the stability of Structure III. On the other hand, solution in Structure I involves no change in the concentration of s,p electrons. Consistent with this description, the solubilities tabulated in the tables show that the metals of the fourth to sixth groups have higher solubilities in Structures I of Mn and Fe than in Structure III and thus stabilize Structure I relative to Structure III. Re, Ru and undoubtedly Tc, and Os, with their intermediate concentration of two s,p electrons per atom are found to be neutral in that their solubilities in both structures are closely the same for Mn. Ru and Os favor Structure III of Fe somewhat over Structure I. The remaining metals, with the exception of Co, favor Structure III over Structure I as they have an excess of electrons which will de-stabilize Structure I by increasing the s,p concentration above 1.5 electrons per atom. Co in its Structure II has the electron configuration d^7sp. Mn in β-Mn undoubtedly displays a mixture of configurations of which d^5sp would be expected to be an important contributor. This is manifested in a very substantial stabilization of β-Mn by addition of Co.

This stabilization greatly reduces the fields of the other two forms and low solubility of Co in Structure III of Mn is due to this competition with the saturating phase of β-Mn structure. Fe does not have any phase with a substantial contribution from an sp electron configuration and Co then stabilizes Structure III over Structure I as expected.

The trends in these tables yield valuable information about the interactions between the various metals and a number of additional comments could be made. However, at this point, the comments will be limited to pointing to the effect of the low internal pressure of Pd and Ag. It was mentioned earlier that these low values are associated with the unusually large promotion energies required to promote d electrons to the p state for these elements. As a result, the solubilities of Pd and Ag are considerably less than would be expected from the basis of electron configuration alone.

In the earlier discussion on the procedure for application of the Engel model, the procedure for predicting the solubility of metals of the seventh to tenth groups in body-centered cubic phases was illustrated by the examples of Tc and Re in Mo and W and Pt in Mo. This procedure is found to yield maximum solubilities in good agreement with the available data. The procedure assumes that the metals with excess electrons will shed their excess electrons to attain the $d^5 s^1 p^{0.5}$ configuration. As noted above, this corresponds to a maximum solubility of 50 atomic percent for Re, 25 atomic percent for Os, 16 atomic percent for Ir, and 12 atomic percent for Pt in a sixth group metal. One must also take into account internal pressure differences and competition of other

phases. Using data for Cr, Mo, and W, the actual solubilities run as follows: Re, 35-43, Os, 10-20, Ir, 10-15, and Pt, 4-10 atomic percent.

It is found that the solubilities predicted on the basis of a $d^5s^1p^{0.5}$ are limits which are often approached, but generally the actual solubilities will lower by an amount which depends upon the difference in internal pressure, the number of intermediate phases, and finally the degree to which the metal with excess electrons is able to lose electrons to attain the d^5 configuration and the degree to which the metal with an electron deficiency can take up electrons to approach the d^5 configuration. Generally the data indicate that the more removed the metals are from one another in the periodic table and therefore the larger the electron transfer required, the larger the deviation from d^5 configuration. Sufficient data are available to map out the configurations to be expected for various combinations of metals.

The mixing of metals which are considerably removed in the periodic table leads to a considerable charge transfer even if they do not quite attain the d^5 configuration. If Ru is dissolved in Hf, for example, the average number of s,p electrons per atom would be below the 1.5 limit for Structure I even in alloys with more Ru than Hf. The average configuration corresponds to d^5s in RuHf although a better description might be $d^{4.5}s^1$ for Hf and $d^{5.5}s^1$ for Ru. Thus a charge transfer of 1.5 to 2 units is expected. Since charges of like sign repell one another, Hf ions tend to become surrounded by Ru ions and vice-versa. This leads to an ordered body-centered cubic structure or the CsCl structure. This ordering leads to additional stabilization of the structure by the coulombic attraction of ions of opposite charge. In Table 8, two body-centered cubic ranges are shown for alloys of Mn

with Rh, Ir, Pd, Pt, and Au. The ranges around 50 atomic percent correspond to ordered CsCl structures[33] and the ranges of few percent solubility correspond to random body-centered cubic structures in which ions of one type are so far removed on an average that no ordering is necessary to avoid coulombic repulsive effects. The charge on the major metal is spread out over many atoms. If one takes an extreme example such as ScPt, one might assign an average electron configuration $d^5 s^1 p^{0.5}$ corresponding to a charge transfer of 3.5 units although the Sc is undoubtedly short of the d^5 configuration and Pt has not dropped down to the d^5 configuration.

One might ask if it is reasonable to expect such large charge transfers and particularly the assumption of a negative charge by Sc of at least two units. Actually, elements can take both positive and negative charges. Thus hydrogen takes a positive charge when it reacts with fluorine while it takes a negative charge when it reacts with an alkali metal. Hydrogen probably takes on a larger actual negative charge than it does a positive charge. In HF, it shares the electron that it has donated and assumes a charge merely due to the polarization of the electron pair bond which draws the electron pair closer to the fluorine nucleus than to the proton. In an alkali hydride, the one negative charge of hydrogen is reduced by polarization of the closed 1 s shell, but lattice calculations indicate that it has a substantial negative charge. In metals with their abundance of electrons, it is much easier for an element to assume a negative charge and one can expect both negative or positive charge for a given element depending upon whether the environment is electron donating or electron trapping. The number of d electrons

that transfer is determined by the additional bonding energy available upon unpairing of d electrons plus the additional coulombic energy that results from the presence of ions. The resulting charge transfer which is limited by the ionization potentials and affinities of the metals is then undoubtedly reduced by polarization of the d electron pair bonds. The problem of characterizing the stability of the structure becomes the same as treating the stability of typical transition metal compounds where there are both ionic and metallic contributions to the bonding. This situation has been discussed[31] for the sulfides of Ce, Th, and U and for other compounds[2,32] of transition metals. These intermetallic compounds with CsCl structure are expected to have similar properties to those of typical compounds of metals with non-metals such as Si, N, P, and S.

The six alkali and alkaline earth metals that we are considering do not form CsCl phases with any of the transition metals. Third group metals are known[32,44] to form CsCl phases with transitions metals of the ninth and tenth groups as well as with metals of the Cu and Zn groups. ScRu is known and other compounds with metals of the eight group are to be expected. Ti forms CsCl phases with Tc, Fe, Ru, Os, Co and Ni while Zr and Hf only forms such phases with Ru, Os, and Co. V forms CsCl phases with Fe, Ru, and Os while Nb and Ta form such phases only with Ru. Beck[12], Dwight[33] and Yao[40] have reviewed the occurrence of CsCl phases and their comments upon the relationship between stability and electron concentration are consistent with the present interpretation in terms of the Engel Correlation. In connection with the discussion of metals taking positive or negative formal charges depending upon the neighboring atoms, it is of interest

to consider the possibility of a reversal of sign of the charge of Sc, for example, in the series of alloys: ScRu, ScRh, ScPd, and ScAg. The Engel theory would predict a negative charge for Sc in alloys where d electron bonding contributes significantly. However, if the alloying metal is far to the right and needs strong d bonding to offset the high promotion energy for d electrons, one may reach an alloy where the p electrons will collapse down into the d shell and Sc need not act as an electron sink. For metals even more to the right, Sc might become positive in a manner similar to the electron transfer in NaTℓ where the Tℓ uses an electron from Na to form a diamond lattice with sp^3 bonding leaving Na^+ held electrostatically. Nevitt[44] has reviewed the behavior of the transition metal phases of CsCl structure and indicates that the elements to the left of the periodic table take a positive charge and that electronic configurations may not be important. In the present discussion, the CsCl phases will be retained as part of the body-centered cubic phase region and will be treated as phases dependent upon electron concentration.

The above discussion illustrates the procedures that can be employed to characterize the occurrence of the body-centered cubic Structure I. The final results after considering competition with other phases are presented for many transition metal systems in the form of phase diagrams at the end of this paper.

V. OCCURRENCE OF THE HEXAGONAL CLOSE-PACKED STRUCTURE II

The hexagonal close-packed structure is not a common one for alloys of the transition metals because of strong competition by structures with overlapping electron concentrations. It has been noted above that the hexagonal close-packed Structure II is to be expected for s,p electron concentrations between 1.7 and 2.1 electrons per atom. The Mg_3Cd or Ni_3Sn and $TiCu_3$ crystal types are also close-packed hexagonal with ordering of the two types of atoms. Their occurrence is considered part of the Structure II range. VCo_3 and $TiNi_3$ crystal types are also included as part of the hexagonal close-packed range although they might be considered as transitional toward the ordered face-centered cubic $AuCu_3$ and $TiAl_3$ crystal types.[12,40,44]

In the earlier discussion, it was noted that the tendency of the transition metals of the first six groups to form structures corresponding to a maximum concentration of d electrons and a minimum concentration of s,p electrons resulted in the occurrence of the body-centered cubic structure for all of those groups although Sr and themetals of the third and fourth groups form the hexagonal close-packed structure at low temperatures. These low temperature hexagonal close-packed phases are of little importance in transition metal alloy systems. When a transition metal to the right of the fourth group, e.g. Pt, is dissolved in a third or fourth group transition metal, e.g. Zr, the Pt will be surrounded by Zr atoms. Since the third and fourth group metals can use their empty d orbitals as electron sinks, the extra d electrons of Pt can be unloaded to maximize the number of unpaired d electrons available for bonding. However, to use these unpaired d electrons, the neighboring

Zr atoms must have sufficient unpaired electrons to bond with the electrons of the Pt. Clearly the body-centered structure I of Zr with a larger number of d electrons per atom will provide better bonding possibilities for the d electrons of the Pt than the hexagonal close-packed Structure II. In agreement with this expectation of the basis of the Engel correlation, it is found almost universally that addition of transition metals to the right of the fourth group in the periodic table stabilizes the body-centered cubic structures of the third and fourth group transition metals relative to the close-packed structures with less d electrons per atom. On the other hand, the addition of non-metals or non-transition metals which can not form d electron pair bonds with the d electrons of the third and fourth group transition metals almost universally stabilizes the close-packed structures. The same tendency to maximize the number of unpaired d electrons per atom at the expense of the s,p electrons is seen in the reverse process of dissolving the third and fourth group metals in transition metals to the right in the periodic table. For example, the fourth groups metals show no tendency to stabilize the hexagonal close-packed structure of Co, nor do they seem to be particularly soluble in Re, although internal pressure differences might be the dominant factor there. Thus it appears that at least 6.7 valence electrons per atom are required before Structure II can be obtained at high temperatures. The instability of the hexagonal close-packed structure for groups seven to nine of the first transition series except for the low temperature form of Co has been discussed earlier. In the second and third transition series, Structure II is found for Tc, Re, Ru, and Os and it is also generally found for alloys of other transition metals with equivalent electron concentrations. The group Tc, Re, Ru, Os and Co with

sp^2 configurations are miscible in all combinations in the hexagonal close-packed structure.

Table 10 presents the composition limits of the hexagonal close-packed structure for alloys of Co. The experimental values obtained from Hansen and Anderko[14] are rather inaccurate when Structure II is stable only at low temperatures because of difficulty in obtaining equilibrium between Structures II and III of Co at low temperatures. The values in parentheses are estimated values. For Mo, W, and V, the 25 atomic percent values corresponds to ordered phases of Ni_3Sn and VCo_3 type[40] which may be separated by a small miscibility gap from the main hexagonal close-packed range. The trends are in agreement with the expectations of the Engel theory. Metals with d^5sp^2 and d^6sp^2 configurations stabilize Structure II. Metals with more electrons increase the electron concentration to the limiting concentration at which Structure II becomes unstable with respect to Structure III. Thus, as metals with more and more electrons are added, the solubility limit decreases. Likewise, metals with too few electrons decrease the electron concentration to the lower critical limit and the fewer the number of electrons per atom of added metal, the lower the solubility limit for Structure II.

To determine the compsoition ranges for various alloys based on metals of the second and third transitions series, it is necessary to establish the number of d electrons per atom associated with the critical limits of 1.7 and 2.1 s,p electrons per atom for Structure II. The procedure has been outlined for the Mo-Pt system in the section discussing the procedure for applying the Engel Model. It was used to fix the limits of Structure I. The data for the fifth and sixth group systems with Re, Os, Ir, and Pt will be used to illustrate the method.

Table 10. Maximum Concentrations in Hexagonal Close-Packed(II) Cobalt in Atomic Percent.

Ni, Pd, Pt	(20)	Cr	40
Rh	(67)	Mo	25
Ir	(75)	W	25
Fe	10	V	(15), 24-32
Ru	100	Nb	5
Os	100	Ta	5
Mn	27	Ti	(15)
Tc	100	Zr	1
Re	100	Hf	(1)

The solubility limit of Structure I for Re in Mo and W corresponds to $d^5s^1p^{0.4}$. If the d shell does not fill up appreciably at the lower end of Structure II, the limit would be expected at about $d^{5.1}s^1p^{0.7}$ or 6.8 valence electrons per atom, which corresponds to a solubility limit of around 20 atomic percent Mo or W in Re. The solubility limit of sixth group metals in Os corresponds to 6.92 - 6.96 electrons per atom. For the low iridium end of the Structure II range, it has increased to 7.0 - 7.1 and for Mo-Pt, it is 7.12 electrons per atom. This indicates a gradual trend from the $d^{5.1}s^1p^{0.7}$ configuration with Re to $d^{5.4}s^1p^{0.7}$ with Pt. The general rule is that there is increasing deviation from d^5, the farther either of the metals is from the sixth and seventh groups. Also the metal of first transition series generally has slightly fewer d electrons than the corresponding metals of the second and third transition series. With Tc, Re, Ru, and Os, the upper limits of Structure II are the pure metals with configurations d^5sp and d^6sp. For Rh and Ir, there is a transition from Structures II to III as the Rh or Ir content increases. With Mo and W, this limit corresponds to $d^{6.2}s^1p^{1.1}$ with only a slightly higher value in Pd and Pt alloys of Mo. These trends are gradual enough to allow rather straightforward predictions of unknown systems.

Table 11 lists the maximum compssitions for which alloys of Tc, Re, Ru and Os retain Structure II. The miscible systems of Te, Re, Ru, Os

Table 11. Maximum Concentrations in Atomic Percent of Solute in the Hexagonal Close-Packed (II) Phases.

Tc and Re Alloys	Ru and Os Alloys
(50) Ni	49 Ni
(10) Pd	40 Pd, Pt
44 Pt	
45 Ir	50 Rh, Ir
25 Rh	
(40) Fe	77 Fe
(25) Mn	51 Mn
20 Cr, Mo, W	50 Cr, Mo, W
5 V , Nb, Ta	30 V , Nb, Ta
4 Ti, Zr, Hf	(25) Ti, Zr, Hf

and Co have not been listed. The values given for Re may also be used for Tc. Likewise, the Ru values may be used for Os as the differences in behavior are smaller than the uncertainties of prediction. The main difference is that the solubility limits for metals of the first and second transition series are closer together for Tc and Ru alloys while the limits for metals of the second and third series are closer together for Os and Ir alloys. Most of these limits have not been experimentally established. Experimental values are available for the Pt, Ir, Mo, W, Nb, and Ta systems of Re, the W, Mo, Cr, Ta, and Nb systems of Ru and Os, and the Ni, Pd, Ir, Fe, and Mn systems of Ru. Values given for any other systems in Table 11 are estimated. References are given later for the systems of the fifth and sixth group metals and systems of the first transition series when drawings of the phase diagrams are given. As diagrams are not given later for the following systems, the references are given here as follows: Ru-Ir and Re-Pt,[34] Ru-Pd,[35,36] Re-Ir,[24,37] Re-Pd and Re-Rh.[37]. The phase diagrams of Tc, Re, Ru and Os with Ni, Pd, Pt, Rh, and Ir are simple systems with a miscibility gap between Structures II and II and with no intermediate phases. The internal pressures are closely enough the same so that no immiscible liquids are expected except possibly for Re-Pd for which the temperature of the liquid range is high enough so that miscibility is expected.

The trends shown in Table 11 are in agreement with the Engel theory. Tc, Re, Ru, and Os with their sp electronic configurations are miscible. Addition of metals to the left reduces the electron concentration to the critical limit for Structure II. The farther to the left, the lower the solubility of a metal as the more electron deficient metals are more effective in reducing the average electron concentration. Addition of metals to the right limits the range of Structure II by increasing the electron concentration to the upper limit. The farther to the right the lower the solubility as the metals with a greater excess of electrons are more effective in increasing the average electron concentrations. Ru and Os with their excess of one d electron can dissolve considerably larger amounts of metals with Structure I than can Tc and Re.

One of the strongest confirmations of the Engel theory is the occurrence of Structure II at intermediate compositions when metals of Structure I are alloyed with metals of Structure III. Wallbaum[41] had recognized the role of electronic configuration in the formation of such hexagonal phases and recent data[16,42] have strongly supported such a view. The composition limits found in these systems correlate with the composition limits found for alloys of Re, Ru, and Os. Table 12 tabulates the experimental or predicted ranges for the hexagonal close-packed Structure II of alloys of Rh, Ir, Ni, Pd, and Pt with metals of Structure I.

Structure II is consistently obtained as an intermediate phase when Ir and Rh are alloyed with metals to the left of group seven. Ni, Pd, and Pt have such as excess of electrons that Structure III persists even with large additions of Structure I metals. Because of the deviation from d^5 configuration when the metals are far removed in the periodic table, the composition ranges for Structures II and III overlap and Structure II becomes unstable with respect to Structure III. The variation of competition between Structures II and III for metals of a given group depends upon relative bonding strengths of d and s,p electrons. Structure II is favored over Structure III in alloys of metals of the seocnd transition series relative to the first and third transition series. Structure II is formed in the Mo-Pt but not in the W-Pt and Cr-Pt systems. However, the phase diagrams given at the end of this paper show that relatively small additions of Mo to either the Cr-Pt or W-Pt are sufficient to stabilize Structure II. Metals of groups four to six form ordered hexagonal close-packed phases with composition AB_3 which are included as part of the range of Structure II. Most values of Table 12 are predicted on the basis of the Engel correlation. References are given for the portion of the data of Table 12 which are experimental at the end of the paper along with the phase diagrams.

No Structure II phases are predicted for any of the metals of the first transition series alloyed with Ni because the range of stability corresponding to hexagonal Co would be too small and would be expected only at low temperature where equilibrium would be difficult to attain

Table 12. Hexagonal Close-Packed Ranges in Atomic Percent of Rh, Ir, Ni, Pd, and Pt.

Mo	50-60 Pd	Cr	35±12 - 70±5	Rh
Mo	28-54 Pt	Cr	35± 7 - 68.5	Ir
		Mo	43 - 82	Rh
		Mo	(36 - 83)	Ir
Nb, Ta, Mo	75 Ni	W	42 - 82	Rh
Zr, Hf	75 Pd, Pt	W	34 - 78	Ir
Ti	75 Ni, Pd	V	(59 - 66)	Rh
		V	(60 - 67)	Ir
		Nb	52-54, 68 - 71	Rh
		Nb	54 - 61	Ir
		Ta	53.5- 62	Rh
		Ta	50 - 55	Ir
		Zr, Hf	(73)	Rh

even if they had a range of stability. Similarily no composition ranges were listed for Mn and Fe alloyed with Rh, Ir, Pd, and Pt. Any such phases would be expected to be stable only at low temperatures. For Mn, it is more likely that α-Mn/or B-Mn would be stabilized rather than a hexagonal phase would form.

The low temperature hexagonal phases of the third and fourth groups have been discussed earlier. They are of little importance in alloy systems except for alloys within each group where complete solid miscibility is expected at temperatures near the melting points.

VI. OCCURRENCE OF THE FACE-CENTERED CUBIC STRUCTURE III

It was noted above in Section III that the face-centered cubic Structure III is found for s,p electron concentrations of 2.5 to 3 electrons per atom. With the exception of low temperature forms of Ca, Sr, and La, which have been discussed above, Structure III is found only among the transition metals for Mn, Fe, the metals of groups nine and ten, and the Cu-Au group. The electron configurations range, on the basis of the Engel correlation, from $d^{4.5}s^{1}p^{1.5}$ for Mn to $d^{7}sp^{2}$ for the tenth group and to $d^{8}sp^{2}$ for the Cu-Au group. These metals with a high d electron concentration have to pay large promotion energies to unpair electrons to make them available for bonding. This requires efficient use of the bonding electrons. If the bonding becomes less effective in an alloy, the atom may return p electrons to the d shell and recover the promotion energy. A clear example is given by the alloying behavior of the metals of the Cu-Au group. In alloys with non-transition metals such as Al, Sn, Zn, etc., which do not provide possibilities for d bonding, the atoms will revert to a $d^{10}s^{1}$ configuration. The platinum metals can be expected to show similar behavior and thus show variable valencies depending upon the environment.

The lowest electron concentration at which one would still expect the III structure is $d^{5}s^{1}p^{2.5}$. This lower limit overlaps the upper limit of Structure II which reaches an average concentration as high as 8.5 electrons per atom for alloys of Mo and W with Rh and Ir corresponding to the configuration $d^{6.4}s^{1}p^{1.1}$ and the actual limits are determined by competition between the two structures as noted in the previous section. Also the combinations of metals with considerably

differing solubility parameters will restrict the solid solution ranges, particularly for alloys of Pd.

Pd, Pt, Rh and Ir are miscible in all combinations at high temperatures. The highest critical temperatures[34] are Pd-Ir, 1476°C, Pt-Ir, 975°C, Pd-Rh, 830°C and Pd-Pt, estimated as 1000°C. Table 13 lists limits of Structure III as well as isolated ordered ranges for alloys of Pd, Pt, Rh, and Ir with metals of Structures I and II. Alloy systems between metals of Structure II and Structure III are not expected to have any compounds other than ordered Structure II and III phases at low temperatures. These diagrams consist of a miscibility gap between solid Structures II and III with miscibility of the liquids. References to sources of data more recent than given by Hanses and Anderko[14] for alloys of Re, Ru, and Os with Pd, Pt, Rh, and Ir are given in connection with Table 11. The other systems of Table 13 are given as phase diagrams at the end of this paper along with references. No other data are available and the remaining information in Table 13 is predicted by use of the Engel correlation.

The competition between Structures II and III is illustrated by the intermediate phases of often relatively narrow range around 75 atomic percent of metals of groups 9 and 10, which have Structure III in the pure state. Alloys of group six metals with group ten metals would yield the electron configuration d^6sp^2 at the composition AB_3 if a maximum number of unpaired d electrons is to be obtained. With platinum, the range of Structure III is well beyond the AB_3 composition. Palladium with its smaller internal pressure has a Structure III range beyond AB_3 for Cr and Mo but can only dissolve 20 atomic percent of W. With Ni neither W or Mo extend the Structure III range up to AB_3 and the use of

Table 13. Limit of Face-Centered Cubic (III) Phases in Atomic Percent of Solute.

Pt		Pd		Rh and Ir	
Ru	60	Ru	16	Ru, Os	(50)
Os	(50)	Os	(15)	Mn, Tc, Re	50
Re	45	Re	(25)	Cr	25-28
Cr	62	Cr	49	Mo	15-20
Mo	42	Mo	39	W	19
W	63	W	20	V	15, VB_3
V	(45)	V	57	Nb	11, NbB_3, $NbIr_{1.1}$
Nb, Ta	36	Nb, Ta	46	Ta	14, TaB_3, $TaIr_{1.5}$
Ti	25	Ti	20	Ti, Zr, Hf	15, AB_3
Zr, Hf	(23)	Zr, Hf	(22)	Sc	$ScRh_3$
Sc, Y	MPt_3	Sc, Y, La	MPd_3		

Formulas are given for ordered phases which are isolated from the main Structure III range.

d electrons by Ni is poor enough to allow formation of ordered $MoNi_3$ with $TiCu_3$ structure, which has the hexagonal close-packed Structure II. The electronic configuration between $d^{7.3}s^1p^{1.7}$ and $d^7s^1p^2$ for pure Ni must have changed to $d^{7.5}s^1p^{1.1}$ if Mo in $MoNi_3$ has the configuration $d^5s^1p^{1.1}$ or to $d^{6.9}s^1p^{1.1}$ if Ni and Mo take the same average configuration. The corresponding $MoPd_3$ of Structure III would have an average configuration $d^{6.3}sp^{1.7}$ and would have more unpaired d electrons available for bonding.

Similarly the fifth group metals can extend the range of face-centered cubic Pd and Pt beyond the AB_3 composition, but $NbNi_3$ and $TaNi_3$ have the ordered $TiCu_3$ type of Structure II. The additional decrease in electron concentration in going to the fourth group results in the $TiNi_3$ type of Structure II for all of the ordered AB_3 compounds except for $TiPt_3$ which has Structure III. $ZrNi_3$ and $HfNi_3$ do not form because of favorable size factors for the Laves phases of compositions between AB_3 and AB_4. $TiPt_3$ of Structure III must be due to the poorer ability of Ti to use its d orbitals as electron sinks. This factor is enhanced in the third group and almost of the ordered AB_3 compounds with Pd and Pt have the $AuCu_3$ type Structure III. La and Ce may be able to fill their d orbitals sufficiently to stabilize $LaPt_3$ and $CePt_3$ in Structure II and the use of unpaired d electrons by Ni is sufficiently poor to allow it to retain sufficient paired d electrons to allow Structure II for $LaNi_3$, YNi_3, and some of the compounds of the first half of the lanthanides and actinides.

The lower electron concentration of the ninth group metals accentuates the competition between Structure II and III and all of the sixth group metals have AB_3 compositions of Structure II with Co, Rh, and Ir although groups six and nine are close enough together so that there is much less ordering effect and the AB_3 compositions are part

of a broad hexagonal close-packed range. The range for Co is considerably reduced and $CrCo_3$ converts to Structure III at high temperatures.

The favorable size factor for Laves phases of Nb and Ta with Co causes reduction of the range of both Structures II and III, but ordered VCo_3 of Structure II forms at low temperatures and transforms to Structure III at high temperatures. For all of the fifth group metals with Rh and Ir, AB_3 phases of Structure III occur separated from the range of Structure III near the pure metals. However, the reduction of electron concentration by addition of more Nb or Ta results in stabilization of the VCo_3 type phase which could be considered intermediate between Structures II and III and is taken as part of the range of Structure II in the phase diagrams of Section VIII and in Table 12. The delicate balance between the two types of structures is illustrated by comparing the Structure II ranges given in Table 12 for Ta-Ir and Nb-Rh with the Structure III ranges given in Table 13. In the Ta-Ir system there are three isolated ranges of Structure III between 56 and 100 atomic percent Ir with the VCo_3 structure between 50.5 and 55 atomic Ir. In the Nb-Rh system there are two isolated ranges of Structure III between 73 and 100 atomic percent Rh and two isolated ranges of VCo_3 structure between 47 and 71 atomic percent separated by a range of the B8 NiAs structure between 63 and 64 atomic percent Rh. This delicate balance of electronic and size factors is shifted in favor of Structure III for the fourth group systems of Rh and Ir by the poorer ability of the fourth group metals to fill up their empty d orbitals. For Co systems, the Laves phases predominate for Hf and Zr systems, but Ti has two regions near $TiCo_3$ of Structure II and

Structure III. For third group metals, $PuCo_3$ has an ordered Structure II and $ScRh_3$ and $ThRh_3$ have ordered Structure III, but generally the Laves phases predominate.

The predictions for alloy systems involving the metals of the first transition series requires recognition of their poorer ability to use their d shells as sinks for electrons. This tends to favor Structure III to lower total electron concentrations than for metals of the other series. The group of face-centered cubic metals Fe, Co, Ni, Rh, Pd, Ir and Pt are miscible in all combinations at high temperatures, and the hexagonal Co and body-centered cubic Fe phases are reduced in stability by addition of any of the other ninth and tenth group metals as discussed in earlier sections. Mn (Structure III) is miscible only with Fe, Ni, and Cu. The reason for the lack of miscibility with Co has been discussed in connection with Table 8 in Section IV. Tables 14-17 gives the limits for the face-centered cubic phases of Mn, Fe, Co, and Ni when alloyed with other metals. Values in parentheses are estimated. References are given in Section VIII of this paper together with phase diagrams for the fourth, fifth and sixth group metal systems as well as for systems of Tc, Re, and Ru. The references for all of the Mn and Fe systesm were given in connection with Table 8 and 9. Data for the remaining systems were obtained from Hansen and Anderko[14]. The trends in the tables have been discussed in connection with the earlier discussion of Tables 8 and 9 and have been found to be generally consistent with the expectations of the Engel theory and the solubility parameters. The main exception is the abnormally high solubility of Cu, Ag, and Au in Ni compared to their solubilities in Co and Fe and their respective solubility parameter differences.

Table 14. Maximum Concentrations in Face-Centered Cubic(III) Manganese in Atomic Percent.

Sc	Ti	V	Cr	Mn	Fe	Co	Ni	Cu
0.3	0.5	0.7	0.85	100	100	4.5	100	100
Y	Zr	Nb	Mo	Tc	Ru	Rh	Pd	Ag
0.5	0.5	0.4	0.6	(5)	37	~33	22	1
La	Hf	Ta	W	Re	Os	Ir	Pt	Au
(0.3)	(0.4)	(0.4)	(0.6)	5	(35)	~33	30.5	25

Table 15. Maximum Concentrations in Face-Centered Cubic(III) Iron in Atomic Percent.

Sc	Ti	V	Cr	Mn	Fe	Co	Ni	Cu
(0.4)	0.7	1.6	13	100	100	100	100	8.3
Y	Zr	Nb	Mo	Tc	Ru	Rh	Pd	Ag
(0.5)	(0.7)	1.7	~2	(15)	29.5	100	100	~0.2
La	Hf	Ta	W	Re	Os	Ir	Pt	Au
(0.4)	(0.5)	0.95	1.0	~16.7	(30)	100	100	8

Table 16. Maximum Concentration in Face-Centered Cubic(III) Cobalt in Atomic Percent.

Ti	V	Cr	Mn	Fe	Co	Ni	Cu
13,20-26	35.2	41	40	100	100	100	12
Zr	Nb	Mo	Tc	Ru	Rh	Pd	Ag
~ 1.3	~5	18.5	(16)	~17	100	100	< 0.1
Hf	Ta	W	Re	Os	Ir	Pt	Au
(1)	~5	17.5	16	~20	100	100	2.5

Table 17. Maximum Concentrations in Face-Centered Cubic(III) Nickel in Atomic Percent.

Ti	V	Cr	Mn	Fe	Co	Ni	Cu
14	43	50	100	100	100	100	100
Zr	Nb	Mo	Tc	Ru	Rh	Pd	Ag
(3)	14	27	(30)	29.7	100	100	~5
Hf	Ta	W	Re	Os	Ir	Pt	Au
(3)	15.4	17.5	(25)	(30)	100	100	100

VII. OCCURRENCE OF Cr_3Si, σ, μ, χ and Other Type Electron Compounds

It was noted above that alloy systems of Structure II and Structure III metals with total electron concentrations between seven and ten electrons per atom are quite simple with no intermediate phases. Alloys of Structure I and Structure II metals with electron configurations between d^5s and d^5sp form a number of complex phases. It is well established that these phases are electron compounds in that electronic concentration is the primary factor which determines their occurrence.[12,20,40,43,44,46,47] For example, when several of the phases are found in the same system, the order with increasing electron concentration is always Cr_3Si, σ, μ, and χ.

The Cr_3Si structure (Strukturbericht type A15) is a cubic structure with each Cr surrounded by ten Cr and four Si while each Si is surrounded by twelve Cr with no near-by Si neighbors. It is also known as the β-W structure after the metastable tungsten phase with W atoms occupying both positions and as the Cr_3O structure. The σ structure (Strukturbericht type $D8_b$) is a complex tetragonal structure with five types of positions with coordination numbers from twelve to fifteen. It is also known as the β-U structure. The μ structure (Strukturbericht type $D8_5$) is a rhombohedral structure closely related to the σ phase.[20] The χ structure (Strukturbericht type A12) is a cubic structure with lattice sites of twelve, thirteen, and sixteen coordination and is also known as the α-manganese structure. Nevitt's recent review[44] presents the available information on these phases and discusses in detail the influence of electronic concentration and size factors upon stability of these phases. Only a brief discussion is necessary here.

The Cr_3Si structure is unusual in having abnormally short distances between the major atoms along mutually perpendicular rows of the atoms.[45] The ordering of the two atoms among the two types of sites is quite complete as the deviation from the three to one ratio is generally quite small. MoTc for which the two atoms are very close together in regard to both size and electronic configuration is an exception. Also the relative size requirements are rather limiting; the radii of the two components do not differ by more than 15 percent.[44]

It is characteristic that the stabilities of the Cr_3Si type phases decrease from the first transition series to the second transition series and this structure is rarely observed with the major metal from the third series. Nevitt[44] has emphasized that the major element of the Cr_3Si type structure does not maintain a spherical shape and that the character of the bonding between like atoms is different from that between unlike atoms. The behavior is reminiscent of the behavior of transition metal ions in various crystal fields. The approach of substituents from directions that minimize repulsive contacts with the unsymmetrical d electron orbitals considerably increases stability. In Section II it was noted that the metals of the first transition series do not make good use of the d electrons in bonding and this was attributed to the small spacial extent of the d orbits compared to the s and p orbitals. With increasing nuclear charge from first to third transition series, the d orbitals become more exposed relative to the s and p orbitals and stronger bonding due to better overlap of d orbitals results for metals of the higher transition series. In the Cr_3Si type structure metals of the first transition series are apparently able to overcome the

relative ineffectiveness of d electron bonding by distortion of the electron cloud to allow better overlap of d orbitals along the direction close contact of the major atom. As the metals of the higher transition series achieve strong d electron bonding without this type of distortion, the stability of the Cr_3Si type structure compared to the competing body-centered cubic Structure I is very much smaller for metals of the third transition series compared to those of the first transition series. This is an important factor in predicting the occurrence of the Cr_3Si type structure.

The competition with Structure I is best illustrated by examining the electron concentration ranges for the Cr_3Si type structure. If one assumes that the transition metal components will attain a d^5 configuration, one can calculate the range of s,p electron concentrations. The 2.0 value for Cr_3Pt corresponding to a d^5sp configuration is the highest s,p concentration observed and is undoubtedly lower due to the Pt retaining more than five d electrons. All other compounds of Cr and Mo have between 1.5 and 1.75 s,p electrons per atom. Thus the Cr_3Si type phase does not intrude into the electron concentration ranges of Structures II or III. The ranges for the compounds of Cr and Mo do not overlap the range for Structure I, but for the fifth group transition metals, the highest electron configuration for a Cr_3Si type phase corresponds to 1.5 s,p electrons per atom in the compounds with Au. On the other hand, Nb_3Os and the Al, Ga, and In compounds of Nb have only 0.75 s,p electrons per atom. V_3Rh and V_3Ga also correspond to only 0.75 s,p electrons per atom, or well within the electronic concentration range of the body-centered cubic structure. This may be due to Nb and V not attaining the full d^5 configuration. If a d^5

configuration is assumed for Ti and Zr, the s,p concentrations for Cr_3Si types phases are less than 1 which would indicate that Ti and Zr do not build up to a d^5 configuration.

Since the ordering of the components between the two sites of the Cr_3Si structure restricts the composition to the three to one ratio, it becomes increasingly difficult to maintain a high enough electronic concentration as the main component is changed from a sixth group metal to a fifth or fourth group metal to compete in stability with the body-centered cubic Structure I. The minor component must contribute a larger number of electrons than for compounds with the sixth group metals. Also the increasing size as one goes from the sixth group to the fourth group together with the restriction in the size ratio eliminates metals of the first transition series as a minor component. The consideration of the various requirements for stability of the Cr_3Si type phase allows one to predict its occurrence. The phase diagrams at the end of this paper show the occurrence of the A15 type structure for transition metal alloys of the fourth to sixth groups with groups eight to ten. The A15 type compounds of Cr and Mo extend outside the transition metals to third and fourth group metals Al, Ga, Si, and Ge. V and Nb can accommodate more electrons and include Al, Ga, In, Si, Ge, Sn, V, As, and Sb in addition to Au and transition metals of the ninth and tenth groups. Ta is reported to form compounds only with Au, Sn, and Sb. Ti forms compounds with third transition series metals from Ir through Au and Hg as well as Sb while Zr is reported only for Au and non-transition elements Al, Hg, Sn, and Pb.[16,44]

In some instances of boder-line stability such as in the Cr-Co system, the body-centered cubic Structure I is stable

down to about 1150°C at the composition Cr_3Co and a possibly stable phase of Cr_3Si type structure could be found only by long annealing at temperatures below 1000°C. It would be of interest to study the stability range of the V_3Co phase as V is replaced by Cr.

In contrast to the Cr_3Si type structure, the σ structure with its variety of lattice positions can shift components from one position to another and can thus be obtained over a range of compositions from 15 to 85 atomic percent. The electron deficient metal can range in size from 93% to 115% of the other component. Thus this structure can be produced for a larger combination of metals with a shift in composition compensating for different electron donating or accepting capacities of the components and occurs generally in phase diagrams between Structures I and II accompanied sometimes by the Cr_3Si type structure at compositions corresponding to lower electron concentrations and by the μ phase for higher electron concentrations. It is interesting that the σ phase occurs in alloys of the Structure I metals and Structure II metals even when the Structure I metal has more total electrons per atom as in alloys of Fe with Tc and Re. It is clear that it is the s,p electron concentration that is controlling. For body-centered-cubic iron, the Engel correlation assigns an electronic configuration $d^{6.5}s^{1}p^{0.5}$. If the same number of d electrons are retained in the σ phase and Re has the configuration $d^{5}sp$, then the average number of s,p electrons per atom for the composition[44] range 46 to 54 atomic percent Fe is 1.75. If one assumes the same number of d electrons for Mn and Fe as in their body-centered cubic structures, namely 5.5 and 6.5, when they alloy

with Tc and Re, the average number of s,p electrons per atom is found to range from 1.7 to 1.8. If one assumes that all metals of the second and third transition series attain the d^5 configuration in the σ phases, one obtains average s,p concentrations falling largely in the range 1.2 to 1.9 with TaAu and NbPd abnormally high at 2.0. In the Ta compounds with Os, Ir, and Pt, the high end of the composition range corresponds to 1.3 to 1.6 s,p electrons per atom, but the low end drops below 1 s,p electron per atom. It is interesting to note that the σ phase Nb_3Al_2 has an average s,p electron concentration per atom of 1.2 if the Nb retains 5 d electrons per atom. In the σ phases of Cr and V with metals of the first transition series, one must assume that Fe, Co, and Ni retain more than 5d electrons per atom in the σ phase to obtain s,p electrons concentrations of 1.2-1.9 per atom. This is consistent with the previous findings for other phases. Thus we conclude that the average s,p electron concentration in the σ phase is generally restricted to the range 1.2 to 1.9 electrons per atom.

Nevitt[44] has reviewed the occurence of the μ phase and the closely related P, R, and δ phases and has pointed out the relation of all of these phases to the σ phase. All of them are characterized by a variety of lattice sites ranging from 12 to 16 coordination and they are undoubtedly stabilized by distribution of atoms of differing size among the various sites, but Nevitt has pointed out that the electron concentration is the primary controlling factor in fixing the stability ranges of these phases. The mixing of different atoms in each of the sites results in excess entropies and these

phases should gain in stability with increasing temperature compared to more ordered phases. Because of the similarity of these structures, it might be expected that the broadening of composition ranges with increasing temperature might result in merging of the phases into one extended homogeneous range. At yet higher temperatures, the competition of the expanding composition ranges of the phases of Structures I and II may cause a reduction in the composition range of the more complex structure region and a breaking up again into limited regions of particular stability. In the phase diagrams which are presented at the end of this report, the distinction between P, R, and μ phases is not maintained and the maximum composition range in which any of these structures might be found is labeled as a μ phase region. The δ phase which is known[44] only for MoNi also should join the μ phase $MoCo_{1.1}$ in the ternary diagram.

The importance of both size and electron concentrations in fixing the stability ranges of the χ phases has been thoroughly covered by Nevitt.[44] To his discussion should be added the factor of competition among the various possible phases. If d^5 configurations are assumed, the average s,p electron concentrations corresponding to the composition ranges of the χ phases are found to be between 1.4 and 2 electrons per atom. There is thus overlap between the electron concentration range of the χ phase with those of Structures II and III on one side and with the σ type phases on the other side. This effect is seen very clearly in the phase diagrams given in the next section where the expanding range of the II structure squeezes out the χ phase of Nb systems, for example, as the other component is changed from a metal of group six to group ten.

Table 18. Maximum Concentrations in α-Mn in Atomic Percent.

Sc	Ti	V	Cr	Mn	Fe	Co	Ni	Cu
(1)	9	(10)	9,~33	100	33	2	4	<0.3
Y	Zr	Nb	Mo	Tc	Ru	Rh	Pd	
<0.5	<1	~3	<5	(10)	12	2	<2	
	Hf	Ta	W	Re	Os	Ir	Pt	
	<1	1	<1	5.5	(5)	<5	<2	

Table 19. Ranges of χ Phases of Tc and Re in Atomic Percent of Solute.

	Sc	Ti	V	Cr	Mn	Fe
Tc	12-15	12-16	(12-18)	(15-20)	(95-100)	(70)
Re		17	(15-20)	——	94.5-100	~69
		Zr	Nb	Mo		
Tc		14-20	14-25	——		
Re		14-20	13-37	17-23		
		Hf	Ta	W		
Tc		12-16	17-20	——		
Re		14-18	20-37	24-27		

Table 20. Maximum Concentrations in β-Mn in Atomic Percent.

Sc	Ti	V	Cr	Mn	Fe	Co	Ni	Cu
1	3	7.5	10.5	100	>25	38	>5	0.3
Y	Zr	Nb	Mo	Tc	Ru	Rh	Pd	Ag
<0.5	1.5	2-3	(5)	(10)	23	<5	<3	<1
La	Hf	Ta	W	Re	Os	Ir	Pt	
(<0.3)	(0.6)	1	<2	(5)	(10)	<6	<3	

Table 13 presents the maximum composition limits for the χ phase upon addition of various metals to Mn which has the χ structure at low temperatures. The trends show clearly the dependence upon electron concentration. Internal pressure differences are also important. The 33 at% Cr composition corresponds to a phase reported[49] to have a structure similar to the χ structure which is separated from the α-Mn solid solution range. Internal pressure differences reduce the solubility of Mo in Mn but a χ phase with 17 at % Mo is formed by adding Mo to Cr-Fe alloys. Ti also forms a similar χ phase and other similar ternary phases can be expected. Table 19 shows the composition ranges for the χ phases of Tc and Re. The phase diagrams of the next section show that the χ phase of Nb and Ta with Tc and Re are so extensive that the seventh group metals can be replaced by metals to the right as far as Ru and Os and almost to Rh and Ir. In addition Fe can exhibit the electronic structure of a body centered cubic metal in alloys with Re yielding a χ phase around Re_4Fe_9 and a similar phase is expected for Tc.

Finally Table 20 shows the composition limits for the cubic β-Mn phase (Strukturbericht Type 13) which also can be considered as another electron compound with about 2s,p electrons per atom. The references to the data of Tables 18 and 20 are the same as those for 8 and 14. These references as well as those for Table 19 will be given in the next section along with phase diagrams. The β-Mn phase requires a slightly higher electron concentration than the χ phase and thus feels even more strongly the competition of the phases of Structures II and III. The same or closely related structure is found[14] for

Ag_3Al, Au_4Al, Cu_5Si, and $CoZn_3$. Among transition metal alloys, it is found in binary systems only for alloys of Mn, but nitrogen stabilizes the β-Mn structure in alloys of Mo with Fe, Co, and Ni. It is also found[44] in the Ni-Mo-O, Cr-Ni-Si, and Fe-Cr-W-C systems.

This stabilizing effect of non-metals is also seen with the cubic Ti_2Ni or $Fe_3W_3C_3$ type structure (Strukturbericht Type $E9_3$) which is related to the σ type structures in containing sites of high coordination number. The binary compounds Sc_2Pd, Ti_2(Co, Ni), Nb_3Fe_2, HfMn, and Hf_2(Fe, Co, Rh, Ir, Pt) are known, but non-metals such as oxygen must be present to stabilize the Ti compounds with Cr, Mn, Fe, Cu, Th, Pd, Ir, and Pt, the Zr compounds with V, Cr, Mn, Fe, Rh, Pd, Ir, and Pt, the Hf compounds with Ni and Pd, the compounds of Mo and W with Mn, Fe, Co, and Ni, and the compound Ta_3Mn_3O. In addition, the ternary compounds Hf_6Ni_2M with M either Re, Os, or Ru are known to exist without non-metal participation. Similar carbides are known[50,51] and nitrides are to be expected. Since this paper is restricted to pure transition metal systems and the Ti_2Ni phase is expected to be uncommon in alloys free of non-metals, the reader will be referred to Nevitt[44] for a review of available information on these compounds and a discussion of the evidence that electron concentrations and atomic size ratios are primary factors. However it might be appropriate at this point to remark briefly upon the general effect of non-metal impurities upon electron-compounds. Hydrogen, oxygen, nitrogen, and carbon act as electron donors[2] in transition metal systems where empty d orbitals are available in contrast to their behavior with metals like the alkali metals or Mg or Al where the non-metals act as electron acceptors. In phase which are below their limiting electron concentrations, the

non-metals usually go into interstitial positions and participate mainly by contributing additional electrons to the metallic bonding system. As the composition of the phase approaches its maximum electron concentration, the ability of the phase to take up the non-metals is expected to be greatly reduced. Due to the charge transfer between the non-metal and metal atoms, there will be ordering effects and coulombic contributions to the bonding energy of the type discussed earlier in connection with the CsCl type structure.

Finally, a brief mention should be made of some additional structures. The $CuAl_2$ (Strukturbericht Type C16) structure is a common structure in metal systems, but in purely transition metal systems it is known only for compounds of third to fifth group metals with Co and Ni such as Sc_2Co, Zr_2Co, Zr_2Ni, and Ta_2Ni. Likewise the common $MoSi_2$ (Strukturbericht Type $C11_b$) structure is reported only for Ti_2Pd, Zr_2Pd, $ZrPd_2$, Hf_2Pd, and $HfPd_2$ and corresponding compounds of Cu, Ag, and Au for purely transition metal systems and the reader is referred to Nevitt's review[44] for a more detailed discussion of these structures.

The tetragonal structure found in the Hf-Re, Zr-Re, and Ti-Mn systems is probably related to the σ structure but seems to form at lower electron concentrations. If the relationship to the σ structure is correct then it might be expected to extend from the Re system of Zr and Hf through Os and Re and possibly as far as Pt. A phase reported at Zr_2Rh might also be of this group.

The orthorhombic CrB B_f type structure is known for Ca with Ge, Sn, and Si; Gd and Dy with Ga and Ge; PrGe; Th with Al, Fe, Co, Rh, Ir, and Pd; and for Ce, Pu, Zr, and Hf with Ni. The Zr_7Ni_{10} phase which also

occurs for Hf is closely related. This structure is expected for Y, La, and many of the other lanthanides and actinides with transition metals of groups eight to ten. It is possible that HfPd, ZrPd, and TiPd might also have this structure. TaRh, NbRh, and NbPd are additional phases of unknown structure which might have the B_f structure although the μ structure is more likely for these last three phases. The FeB structure is known for Gd and Dy with Ni and Pt and for CeCu. It is expected mostly for the middle and second half of the lanthanides with the tenth group transition metals and the first half of the lanthanides with Cu and Au. A large fraction of the AB compounds of the third group metals and lanthanides and actinides with transition metals of the iron and platinum groups and of the Ag, Cd, and In groups are of the CsCl structure which has been discussed earlier. The competition between these structures is determined by electronic configuration and relative sizes.

The B19 AuCd or MgCd structure is known for MoPt, NbRh, and VPt. It probably extends to VIr and VOs and may also be the structure of TaPt and NbPt. It covers a range of electron concentrations higher than one would expect for the μ phases and slightly less than for Structure II and occurs in systems where the χ phase is excluded. The B8 NiAs structure, which is a common system, is rare for purely transition metal systems and only in the Ta-Rh system is there a phase which might be described as a distortion of the NiAs structure.

VIII. Multicomponent Phase Diagrams of the Transition Metals

The previous sections have used an inductive analysis of the available phase diagram data for the transition metal systems to establish a correlation between phase behavior and s-p or d electron concentrations, internal pressures, and radius ratios. The rules illustrated in the previous sections allow one to translate known phase behavior into an electron distribution between s-p and d electrons which becomes the primary parameter for predicting behavior in unknown systems. The following phase diagrams represents the combination of known data together with the predictions of the Engel correlation.

It is not feasible to present more than a small fraction of the two billion multicomponent phase diagrams of the thirty metals being considered in this paper. Fortunately, the phase behavior, at least at high temperatures, is quite simple for the various combinations of the eighteen metals of the first six groups and no diagrams are necessary to supplement the discussion of Section IV. Likewise the diagrams for combinations of the metals of the seventh, eighth, ninth, and tenth groups are simple enough so that no diagrams are considered necessary to supplement the detailed discussions of these diagrams in the previous sections except for combinations of Tc, Re, and Ru with the first transitions series metals Mn to Ni. Of the remaining systems, it has been chosen to represent diagrams for combinations of metals of the fourth to sixth groups with metals of the seventh to tenth groups.

All diagrams [presented] are projections of phase regions over the entire temperature region up to the solidus temperatures. The composition ranges given thus represent the maximum ranges at the optimum temperature for

each phase. The phases shown do not necessarily exist at a common temperature. When the maximum composition ranges of ajoining phases overlap to a large extent, the limiting composition range of the low temperature form is indicated as a dotted line. In some instances where the maximum ranges just barely overlap, the drawings do not show any overlap to avoid any confusion in regard to identification of the phases. I, II, and III identify the body-centered cubic, hexagonal close-packed, and face-centered cubic phases. L represents any of the five Laves phases of ideal composition AB_2 or AB_5. χ represents the α-manganese structure. σ will be used for the σ phase region and μ will be used for the μ, P, R, and γ phases. For the remaining phases, the Strukturbericht designations are used: A15 for Cr_3Si type, C16 for $CuAl_2$ type, C11b for $MoSi_2$ type, and $E9_3$ for Ti_2Ni type, etc. as shown in Table 21.

A simplified method of representing multicomponent phase diagrams is used. Figure 10, the diagram for alloys of Ta with W, Re, Os, Ir, and Pt, can be used to illustrate the method. The horizontal scale gives the composition in atomic percent with 100% Ta on the left and 100% of the alloying metal on the right. The top horizontal line represents the binary Ta-W system. A horizontal line at the level of the symbol Re represents the binary Ta-Re system, etc. A horizontal line half-way between Re and Os, for example, would represent an equimolal mixture of Re and Os mixed with Ta with 100% Ta at the left and 0% Ta at the right. The various horizontal lines that can be drawn between Re and Os correspond to various ratios of Re and Os in alloys with Ta. For most of the systems chosen the internal pressures and sizes of the atoms are close enough together so that different combinations of metals yielding the same electron concentration show

Table 21. Symbols Used in Figures to Designate Phase Regions.

Figure Designations	Crystal Type	Structure Designation	
I	body centered cubic	A2 and B2	
II	hexagonal close packed	A3, DO_{19}, DO_{24}, $TiCu_3$	
III	face centered cubic	A1, $L1_2$	
III	tetragonal $TiAl_3$	DO_{22}	
	tetragonal and CuAu	$L1_0$	
L	cubic $MgCu_2$	C15	Laves phases
L	hexagonal $MgZn_2$	C14	
L	hexagonal $MgNi_2$	C36	
L	face centered cubic UNi_5	$C15_b$	
L	hexagonal $CaCu_5$	$D2_d$	
A15	cubic Cr_3Si	A15	
σ	tetragonal β-U	$D8_b$	
∅	tetragonal HfRe	∅	
μ	rhombohedral W_6Fe_7	$D8_5$	
	rhombohedral and $Mo_7Fe_2Ni_5$	P	
μ	orthorhombic MoNi	δ	
	orthorhombic and Ti_2Mn_9	R	
χ	cubic α-Mn	A12	
β	cubic β-Mn	A13	
$E9_3$	face centered cubic Ti_2Ni	$E9_3$	
$C11_b$	tetragonal $MoSi_2$	$C11_b$	
C16	tetragonal $CuAl_2$	C16	
B_f	orthorhombic CrB and Zr_7Ni_{10}	B_f	

approximately the same phase behavior. Thus the horizontal line half way between Re and Os intersects the phase boundaries at compositions corresponding to the behavior of a system of Ta mixed with a equimolal mixture of Re and Os. This same horizontal line also represents the mixing of Ta with an equimolal mixture of W and Ir, the mixing of Ta with an alloy containing 25% each of W, Re, Os, and Ir or any mixture of W, Re, Os, Ir, and Pt which averages out to 7.5 valence electrons per atom. The major difference between binary systems and multicomponent systems of the same electron concentration will be an increased stabilization of phases with non-equivalent sites such as σ and χ phases compared to phases with equivalent sites such as face-centered cubic, for example. With this use of the diagrams, each diagram corresponds to a large number of multicomponent diagrams. This use of the diagrams for multicomponent systems works best for metals of the third transition series and poorest for metals of the first transition series.

The reference numbers after each binary line of the diagram refer to the latest publications or compilations which in turn give references to the complete bibliography for work done on the binary system. If a complete phase diagram over the entire temperature range below the solidus curve is available, the reference number is marked with a double star**. If the published diagram is incomplete, but substantial data are available on the effect of temperature on the composition ranges of the phases, the reference number is marked with a single star*.

For structures with a number of non-equivalent sites such as the such as the σ, μ, χ and related phases, it is expected that the range of stability is smaller in binary systems than in ternary of higher components systems. This is indicated by a narrowing of the phase region at each binary intersection, e.g., the σ phase region of Nb with W, Re, Os, Ir, and Pt in Fig. 11. If equi-molal alloys of Pt and Os are mixed with Nb, it is expected that a wider σ phase region would be obtained than if Ir were mixed with Nb. For the multicomponent systems, the expected σ phase region would be the envelope of the indicated boundaries without any flex points.

The curves have been slightly distorted in some instances to avoid crossing where overlapping is small to simplify the presentation of the figures. In instances where metals such as Mn and Fe have several structures, the diagram has been simplified by omitting the areas of the structures of small extent as this information is given in Tables 8, 9, 14, 15, 18, and 20. The Structure II ranges of the fourth group metals have not been indicated as they are very small in all the diagrams. In a few instances the miscibility gap between body-centered cubic Mn and Fe has been omitted for simplicity.

The use of the dotted lines might be illustrated by Fig. 26. The σ phase of Mo forms a continuous range from Mn to Co. However, in the center portion for compositions in the vicinty of Fe, the σ phase is unstable at high temperature with respect to the disordered body-centered cubic phase. The dotted lines indicate the compositions which are stable only at low temperatures. The structure II range starting at pure Co is bounded by dotted lines except in the vicinity of $MoCo_3$ as it is stable

only at low temperatures for most of its range and changes to Structure III at high temperatures. Structure III which is the high temperature form for Ni and Co is shown bounded by a solid line which changes to dotted between Co and Fe where structure III transforms to Structure I at high temperatures. The boundary becomes solid again between Fe and Mn. The boundary of Structure I becomes dotted as it approaches the 25Fe75Co composition since Structure III is the stable high temperature form with less than 10 atomic percent Mo. Similarly, the χ region is bounded by solid lines in the region of 10-20 atomic percent Mo but becomes dotted at lower concentrations where β-Mn becomes the form stable at high temperatures.

In a composition region bounded by solid lines, there is only one structure possible. Composition regions bounded by dotted lines have two or more structures. The structures possible for a dotted region can be determined by noting the phase designations in the regions bounded by solid lines and following the extensions of the solid lines as they change to dotted lines. Region bounded by dotted lines will not have a phase designation if the phase has any composition range which does not transform to another solid phase before reaching contact with the liquidus curve and thus will extend into a range bounded by solid lines.

Referring again to the lower right hand corner of Fig. 26, only those portions of the composition regions of Structure II and III where one phase forms are labeled. Structure III forms at high temperatures for all compositions to the right of the solid line starting at 72 atomic percent Ni. This line continues as a dotted line through the Structure I region between Fe and Co, but all compositions to the right of this line can form Structure III. Structure II can form between the two lines starting on the

right hand side at 10Fe90Co and 20Ni80Co, respectively, and ending at the bottom at 74Ni26Mo and 76Ni24Mo, respectively. Only in the portion that extends to the left of the Structure III boundary and which is bounded by solid lines is Structure II not converted to Structure III at high temperatures. In most instances, the identification of the phases possible in these overlapping areas is quite obvious.

In the preparation of these figures, the available experimental data have been treated in three ways. First there are quite complete data of unquestioned reliability for some systems and this is presented unaltered in the figures. In other instances, several conflicting observations have been reported in the literature and the Engel correlation has been used to select from among the conflicting data. In other instances, single investigations have been reported which appear to be in error. When some internal inconsistencies are apparent which allow rejection of such data, this has been done. However, when there is no substantial basis for rejection of the data, they have been presented in the figures as reported. In very many instances, no data have been reported and the Engel correlation has been used to predict existence of phases and their ranges, but this has been done in a conservative manner and extrapolations have not been carried too far from existing data; so that these figures can be used as representative of the existing experimental data.

However, the discussion in the text and the methods described there can be used by the reader to make more extended extrapolations and to extend this treatment outside the group of 30 metals treated in the figures, tables, and discussion of this paper. To aid in such extentions, the internal pressure data which were discussed in Section III are tabulated

in Table 23 and the tables of crystal structures of the elements and enthalpies of sublimation of the elements from reference 2 are given in Table 22 and 24 at the end of this paper.

Acknowledgements

A number of people have played an important part in the production of this paper. First, of course, the key correlation of the approach used in this paper is due to the imaginative inductive insight of Niels Engel. Secondly, this paper would never have been possible without the critical evaluation and compilation of metal phase studies up to 1958 by M. Hansen and K. Anderko. Orginally, it was planned to merely present the final phase diagrams with only a brief discussion of the details of the methods used to predict them. The present lengthy and more detailed paper is due to the prodding by John Chipman during his stay at Berkeley to obtain a paper that could be used by metallurgists and physicists without extensive chemical background who might wish to carry on these methods to other systems. Another factor which lead to the development of this paper was the environment of the Inorganic Materials Research Laboratory in which the divergent views of metals from the points of view of chemistry, physics, and metallurgy are being amalgamated and where detailed knowledge of phase diagrams is necessary for proper design of a variety of experiments.

The Division of Research of the U.S. Atomic Energy Commission has provided the funds for this work, but the contribution has gone beyond that. In particular Donald K. Stevens, Assistant Director of Research for Metallurgy and Materials Programs has personally stimulated and encouraged this work and it is hoped that this paper will be an important contribution of the Atomic Energy Commission to the practical development of new materials.

Finally, the help of Diane Ota in the preparation of the manuscript through many revisions is acknowledged.

Fig. 1

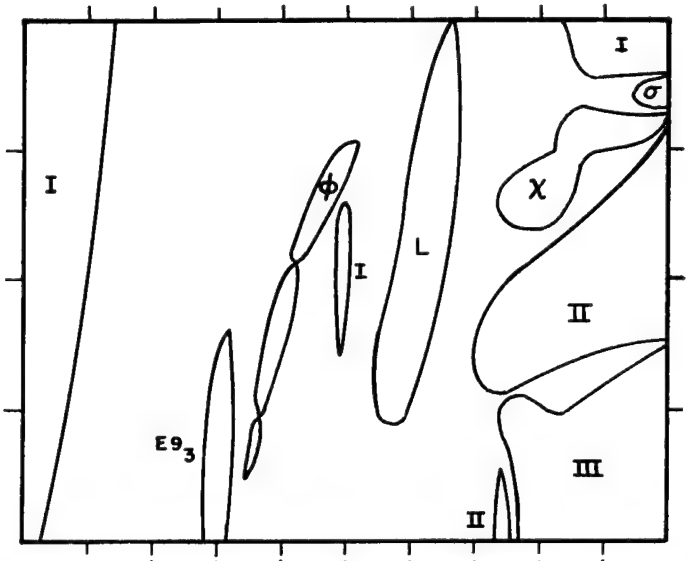

Hf

W 106 **
Re 107 *
Os 44
Ir 44, 88
Pt 44

Fig. 2

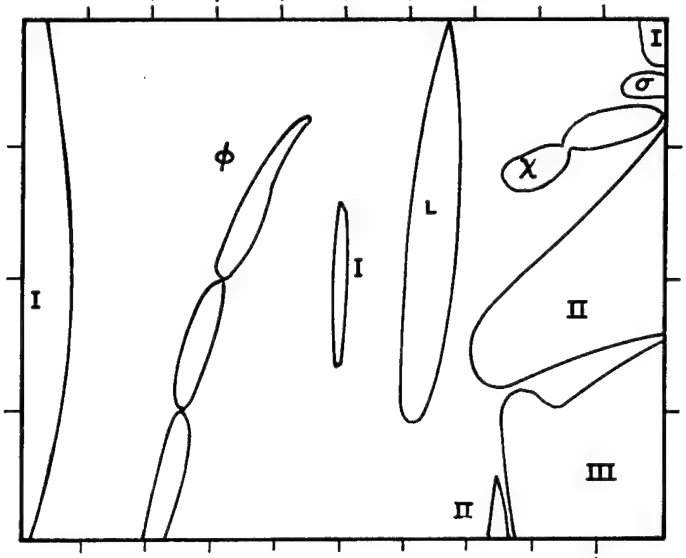

Zr

W 14 **
Re 44, 108 *
Os 44
Ir 44, 52
Pt 44, 52

Fig. 3

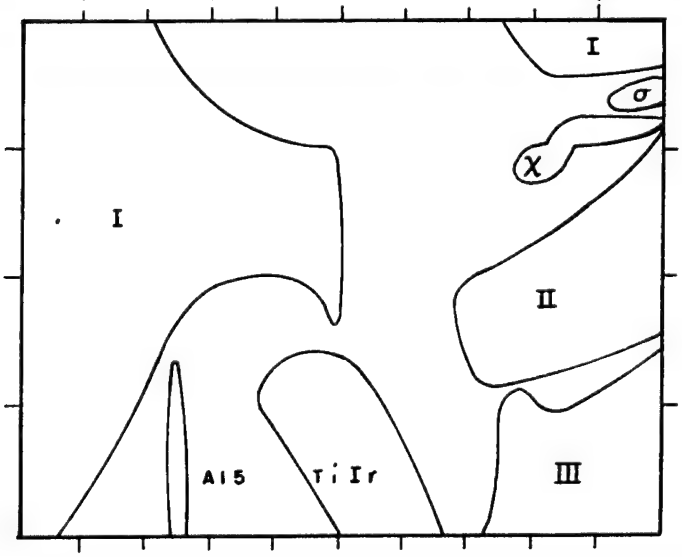

Ti

W 14 **
Re 53 *, 108 *
Os 14
Ir 48 *
Pt 14, 44

MUB-2026

Fig. 4

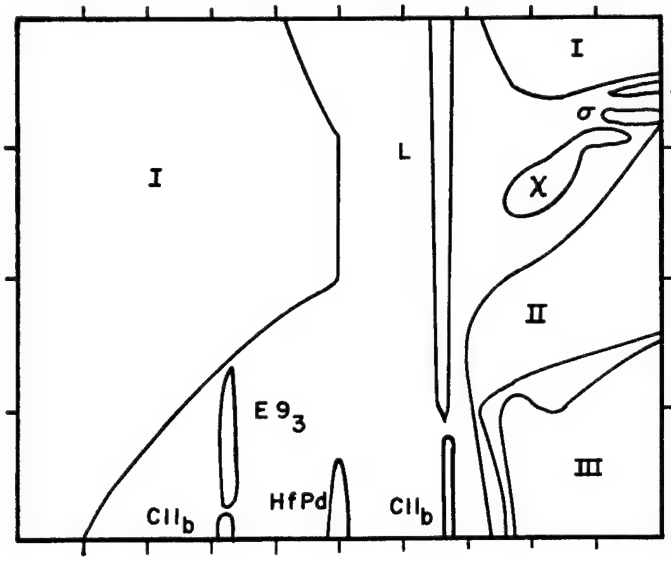

Fig.5

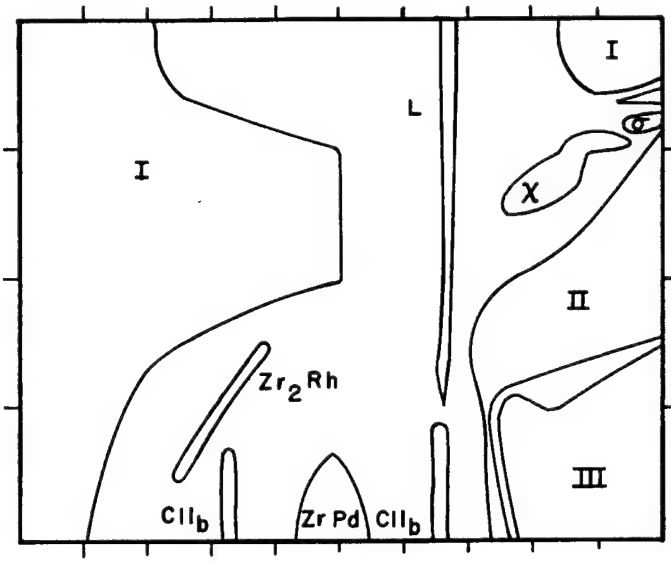

Fig.6

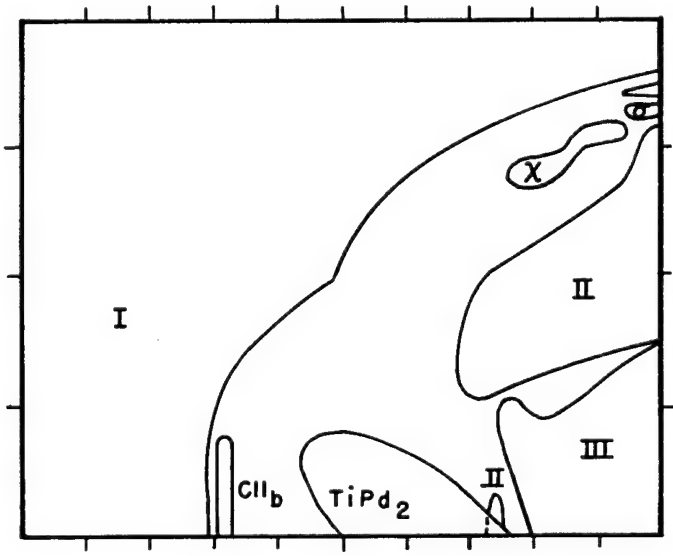

MUB-2027

Fig. 7

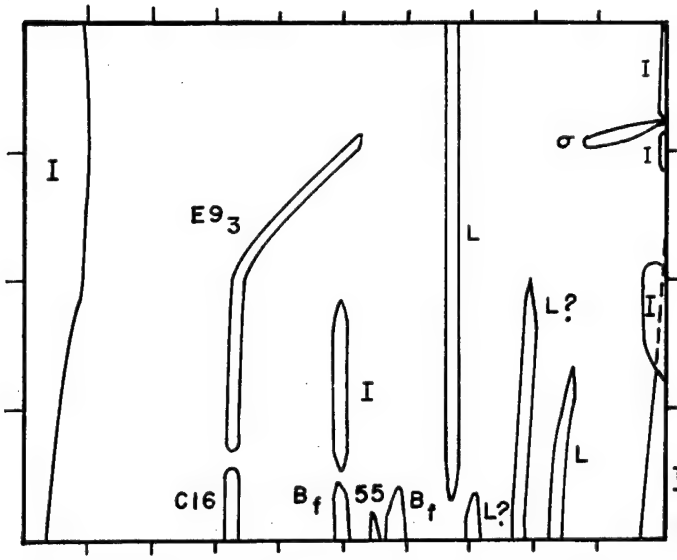

Fig. 8

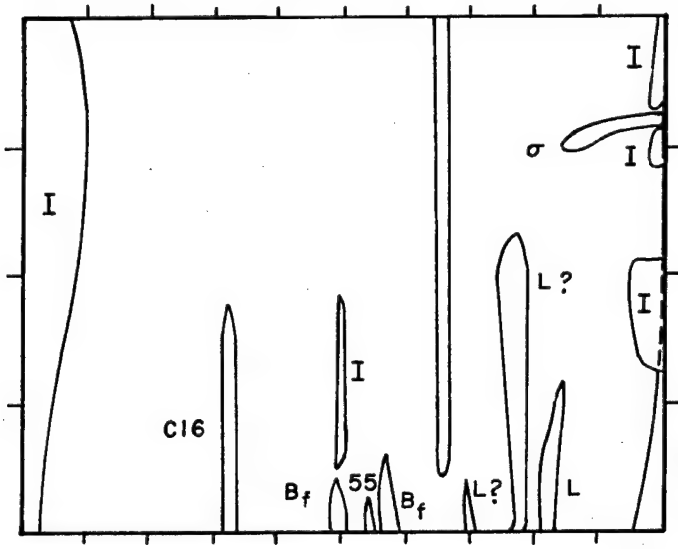

Fig. 9

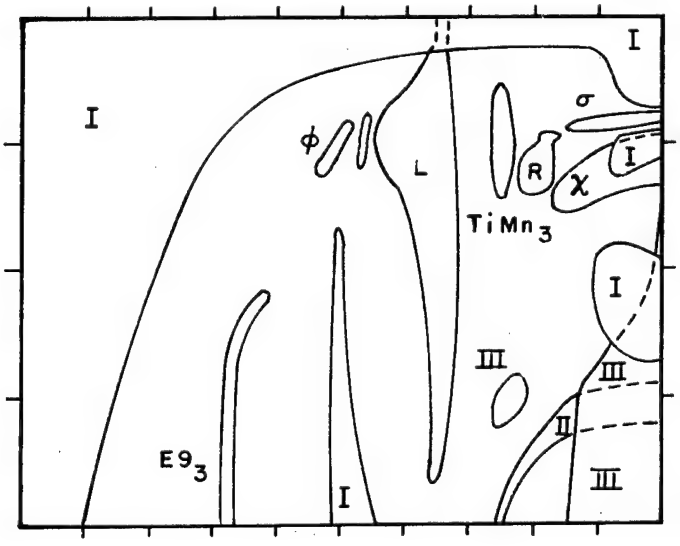

MUB-2028

,Cb,Ta,W,Cr,V,Al,Mg,ES,SS,NiB,
,Be,Ti,Pt

Fig. 10

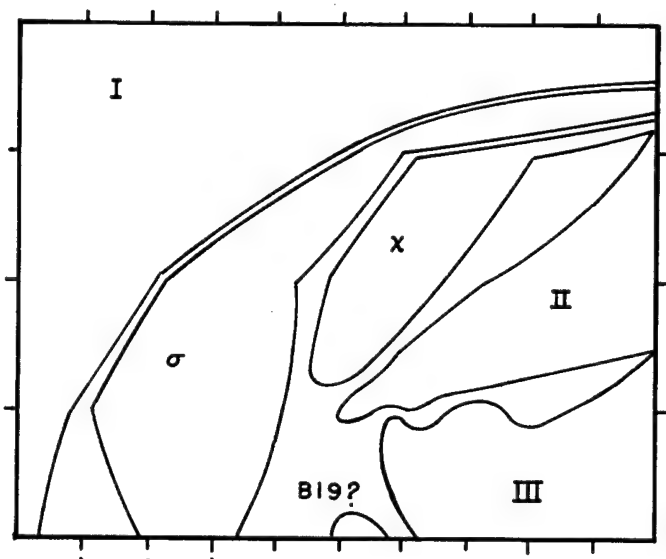

Fig. 11

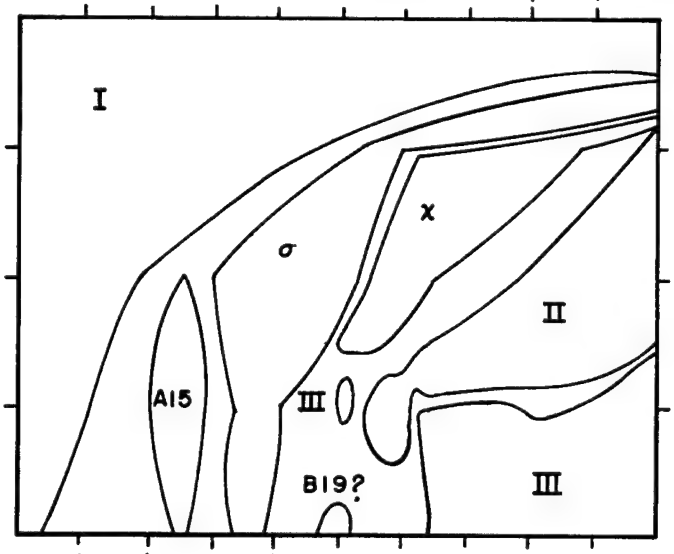

Fig. 12

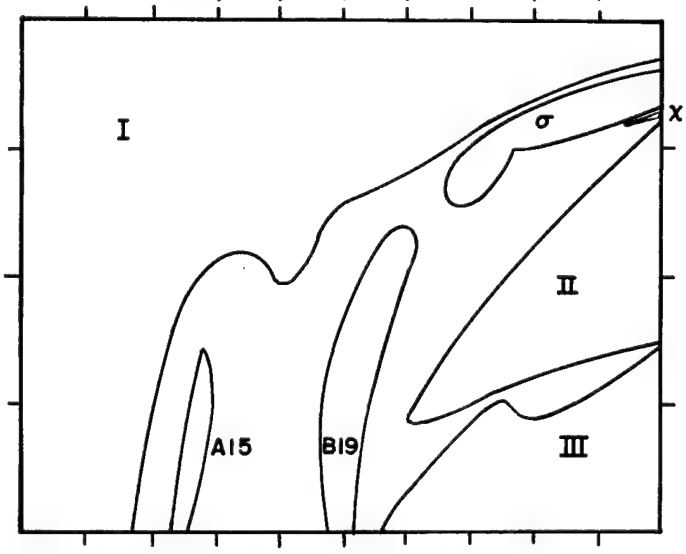

MUB-2029

Fig. 13

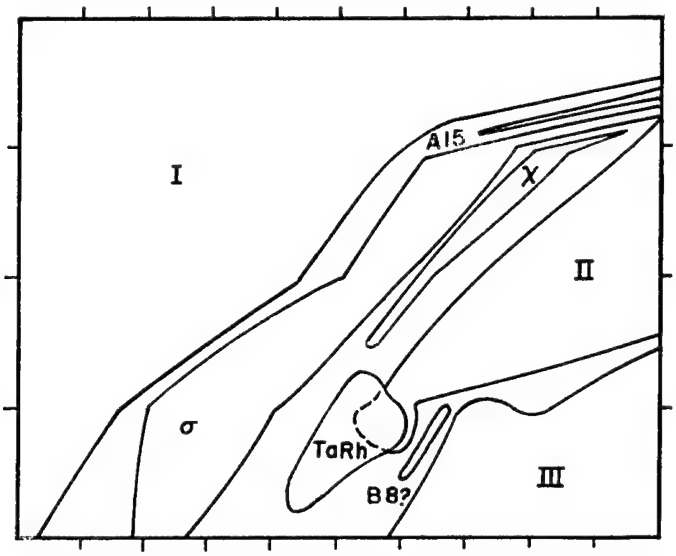

Fig. 14

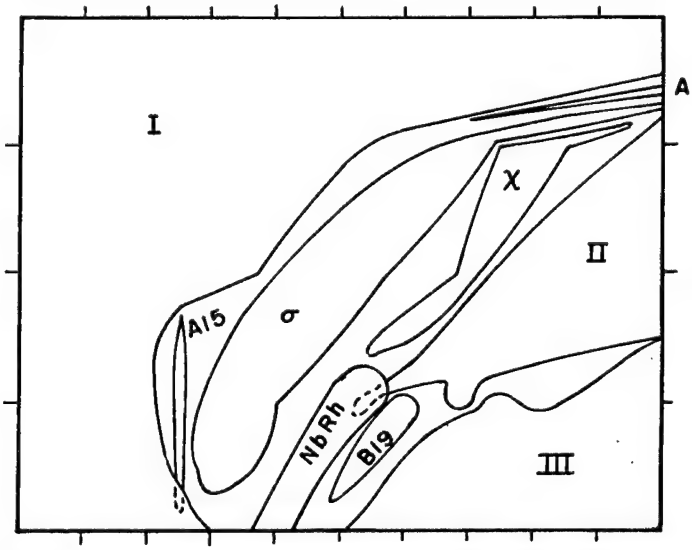

Fig. 15

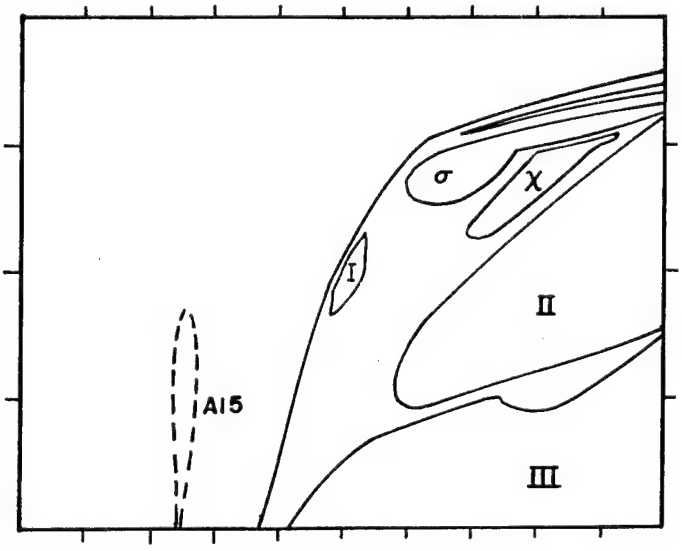

MUB-2030

Fig.16

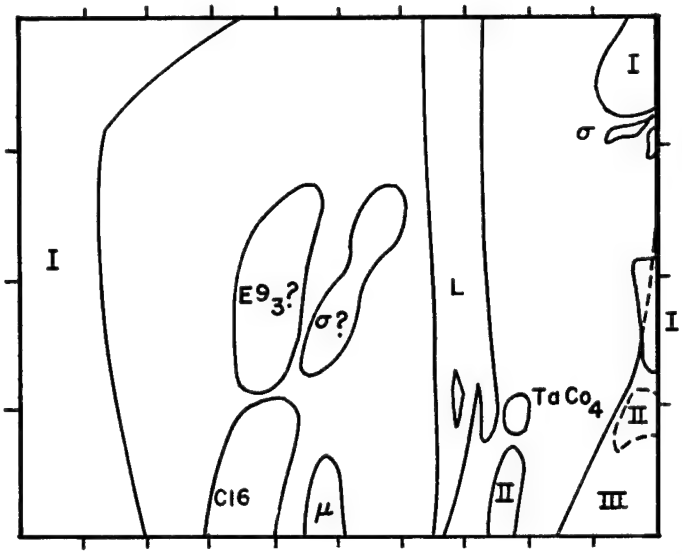

Fig. 17

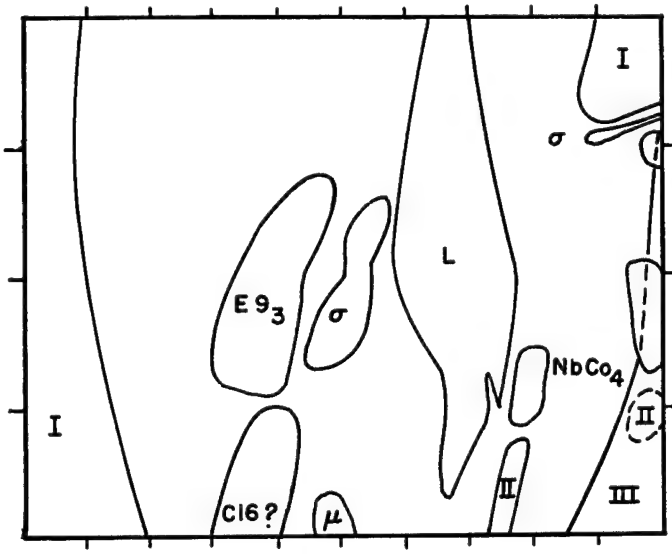

Fig. 18

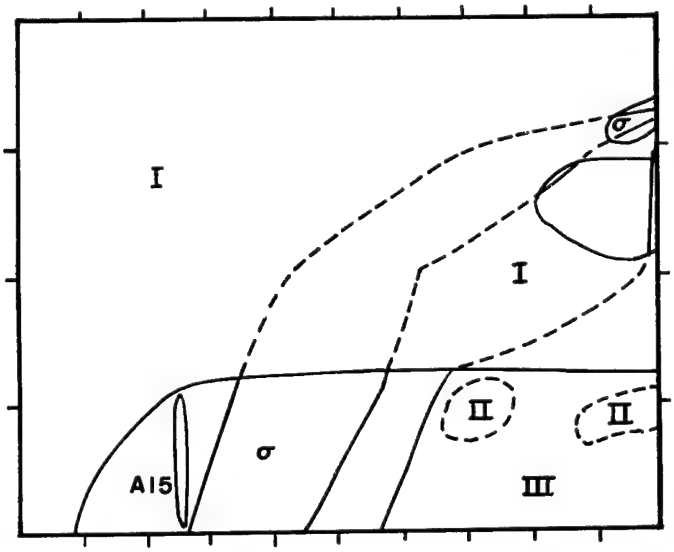

MUB-2031

Fig. 19

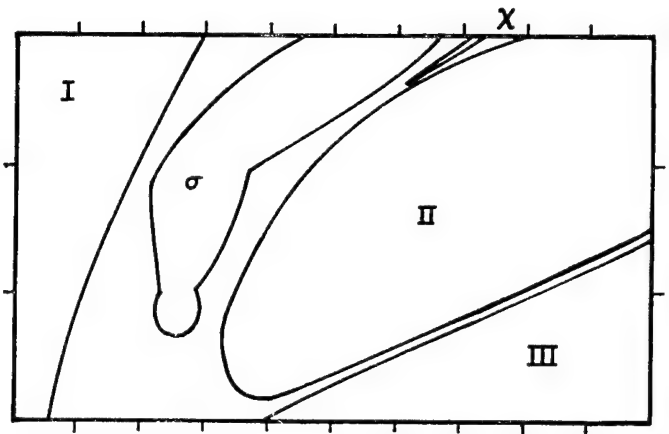

Fig. 20

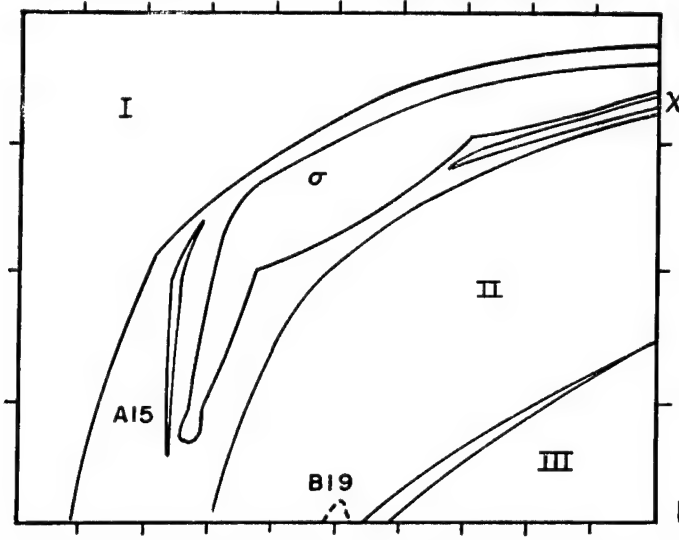

Fig. 21

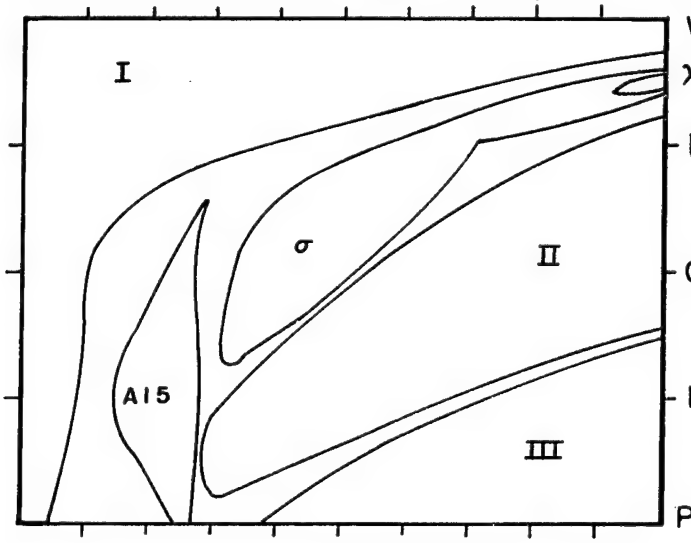

MUB-2032

Fig. 22

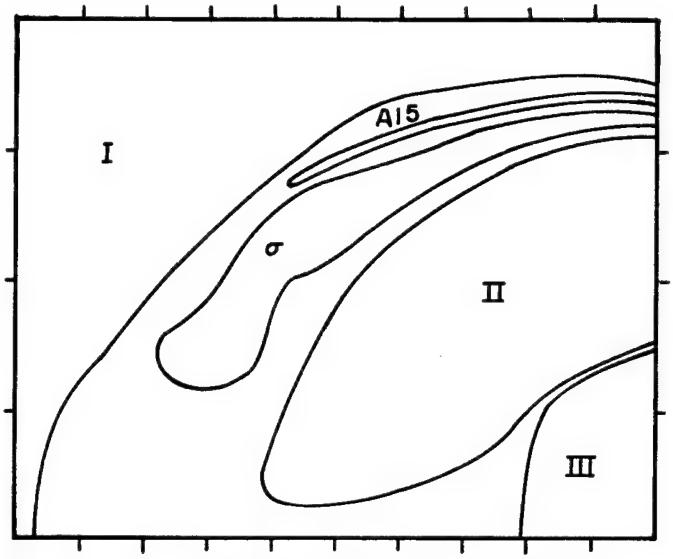

Fig. 23

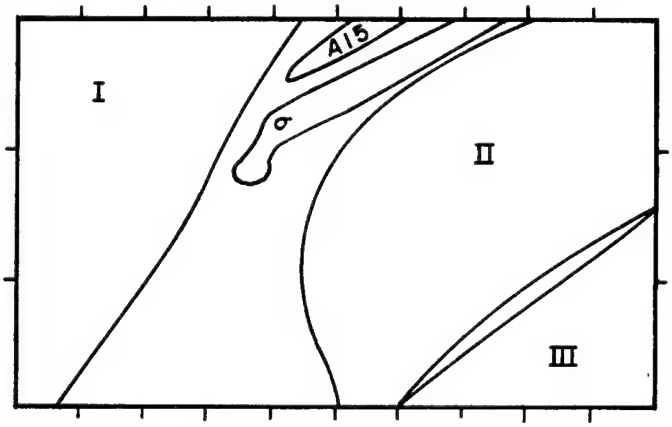

Fig. 24

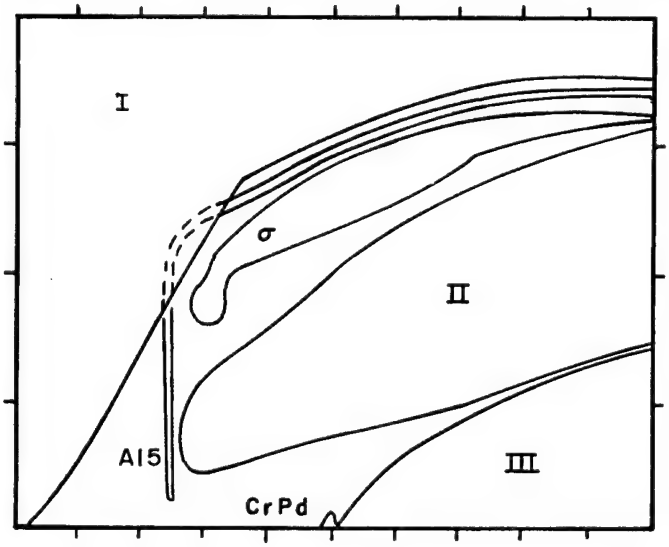

MUB-2033

Fig. 25

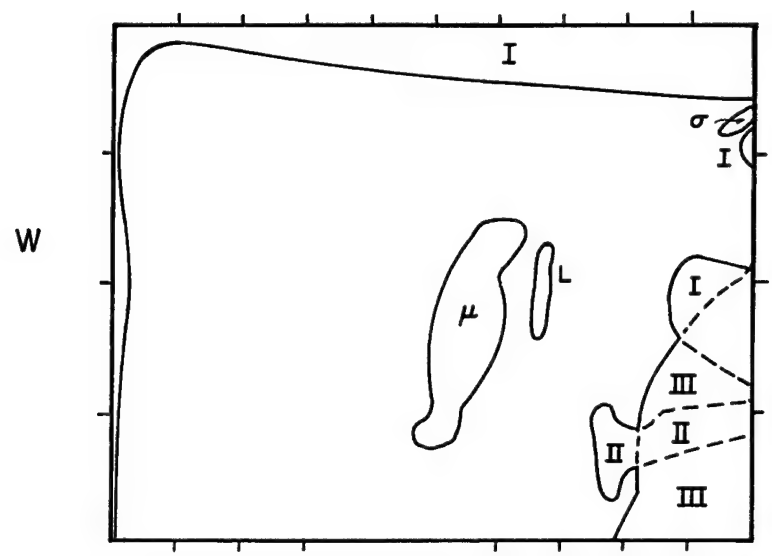

Fig. 26

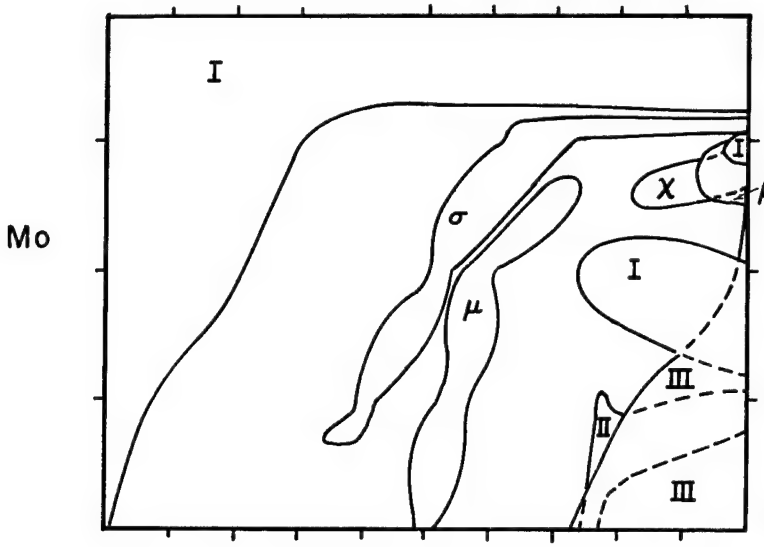

Fig. 27

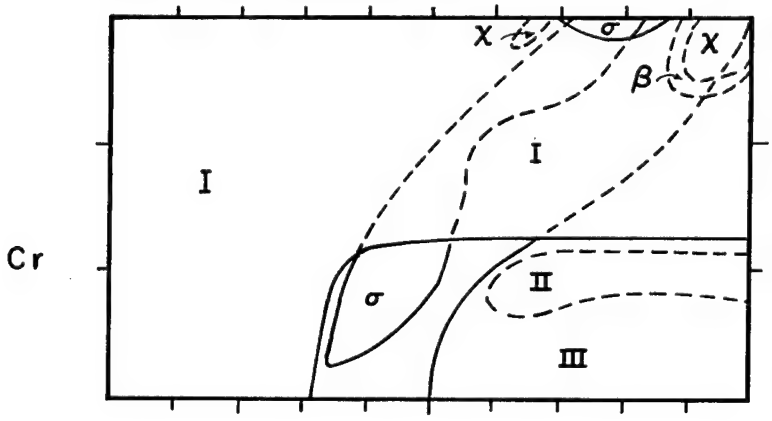

MUB-2034

Fig. 28

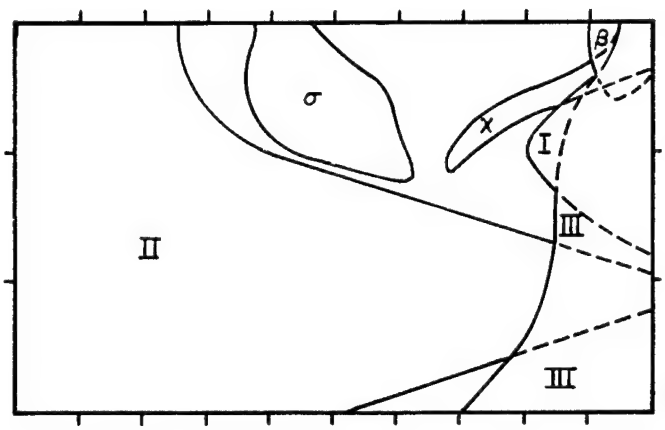

Fig. 29

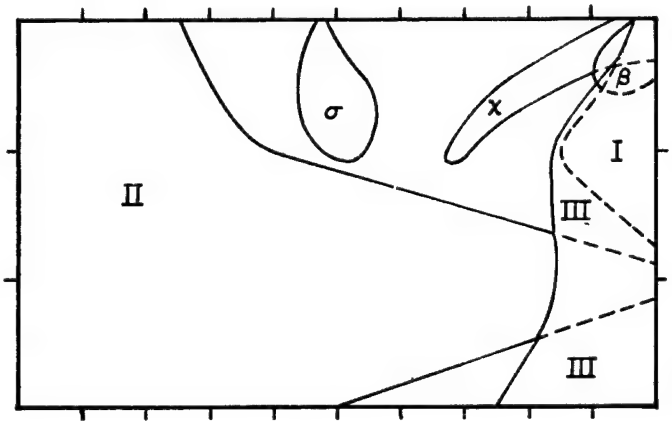

Fig. 30

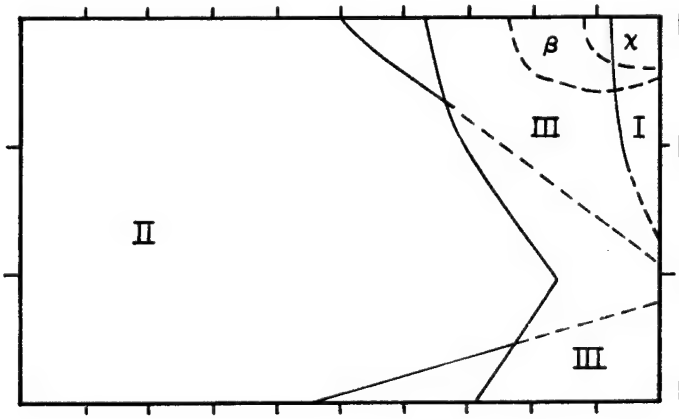

MUB-2035

TABLE 22

Heat of Atomization of the Solid Elements in Kilocalories/Gram Atom at 298.15°K or at the Melting Point, Whichever Temperature Is Lower

Li	Be	B										C	N	O	F	Ne
38.4	77.9	130										170.9	113.7	60.4	19.7	0.50
Na	Mg	Al										Si	P	S	Cl	Ar
25.9	35.6	77.5										108	79.8	66	32.2	1.84
K	Ca	Sc	Ti	V	Cr	Mn	Fe	Co	Ni	Cu	Zn	Ga	Ge	As	Se	Br	Kr
21.5	42.2	88	112.7	123	95	66.7	99.5	101.6	102.8	81.1	31.2	69	90	69	49.4	28.1	2.55
Rb	Sr	Y	Zr	Nb	Mo	Tc	Ru	Rh	Pd	Ag	Cd	In	Sn	Sb	Te	I	Xe
19.5	39.1	98	146	173	157.5		153	133	91	68.4	26.75	58	72.0	62	46	25.5	3.57
Cs	Ba	La	Hf	Ta	W	Re	Os	Ir	Pt	Au	Hg	Tl	Pb	Bi	Po	At	Rn
18.7	42.5	102	160	186.8	200	187	187	159	135.2	87.3	15.32	43.0	46.8	49.5	34.5		
Fr	Ra	Ac														

Ce	Pr	Nd	Pm	Sm	Eu	Gd	Tb	Dy	Ho	Er	Tm	Yb	Lu
97 ±3	80 ±4	77 ±1		50 ±3	42 ±3	84 ±2	80 ±7	62 ±4	70 ±3	66 ±4	58 ±2	40 ±5	95 ±10
Th	Pa	U	Np	Pu	Am	Cm	Bk	Cf	Es	Fm	Md		Lw
136.6	126	125	105	92	66								

Table 23

Low Temperature Solubility Parameters of Solid Metals, $\left(\frac{\Delta E}{V}\right)^{1/2}$ in $cal^{1/2}/cc^{1/2}$.

Na	Mg	Al	Si								
33.	50.	88.	94.								
K	Ca	Sc	Ti	V	Cr	Mn	Fe	Co	Ni	Cu	Zn
21.5	40.	76.	103.	121.	114.	95.	118.	124.	124.	107.	58.
Rb	Sr	Y	Zr	Nb	Mo	Tc	Ru	Rh	Pd	Ag	Cd
18.5	34.	70.	102.	126.	130.	135.	135.	126.	101.	81.5	45.
Cs	Ba	La	Hf	Ta	W	Re	Os	Ir	Pt	Au	Hg
16.	34.	67.	108.	131.	146.	146.	148.	136.	122.	92.	32.

TABLE 24

Crystal Structures of the Elements[a]

Li I	Be II	B * *											C IV > = [f]	N ≡ [b]	O = [b]	F — [c]
Na I	Mg II	Al III											Si IV	P ↗ [e]	S ↙ [d]	Cl — [c]
K I	Ca I III	Sc I II	Ti I II	V I	Cr I	Mn I III β χ	Fe I III I	Co III II	Ni III	Cu III	Zn II	Ga All	Ge IV	As ↗ [e]	Se ↙ [d]	Br — [c]
Rb I	Sr I II III	Y I II	Zr I II	Nb I	Mo I	Tc II	Ru II	Rh III	Pd III	Ag \ III	Cd II	In (III)[g]	Sn A5 IV	Sb ↗ [e]	Te ↙ [d]	I — [c]
Cs I	Ba I	La I III II	Hf I II	Ta I	W I	Re II	Os II	Ir III	Pt III	Au III	Hg A10	Tl I II	Pb III	Bi ↗ [e]	Po	At
Fr	Ra	Ac														

Ce I III II	Pr I II	Nd I II	Pm	Sm I (II)[g]	Eu I	Gd I? II	Tb I? II	Dy II	Ho II	Er II	Tm II	Yb I III	Lu II
Th I III	Pa *	U I σ A20	Np I? **	Pu I * III **	Am ? II	Cm ? II	Bk	Cf	Es	Fm	Md		Lw

[a] I: Body centered cubic, A2. II: Hexagonal close packed, A3. III: Cubic close packed, A1. IV: Diamond, A4. Asterisk denotes complex structure. [b] Diatomic molecules with double or triple bonds. [c] Diatomic molecule with a single electron pair bond. [d] Atoms which form two single bonds per atom to form rings or infinite chains. [e] Three single bonds per atom, corresponding to a puckered planar structure. [f] The graphite structure where one resonance form consists of two single and one double bond per atom. [g] Parentheses indicate slight distortions.

REFERENCES

1. N. Engel, Kem. Maanedsblad, No. 5, 6, 8, 9, and 10 (1949)(in Danish). A mimeographed manuscript in English was circulated in this country in the late forties and early fifties. A brief summary is given in Powder Metallurgy Bulletin 7, 8 (1954).

2. Leo Brewer, Thermodynamic Stability and Bond Character in Relation to Electronic Structure and Crystal Structure, paper in Electronic Structure and Alloy Chemistry of the Transition Elements, Ed. Paul A. Beck, Interscience, New York, 1963.

3. J. H. Hildebrand and R. L. Scott, Solubility of Nonelectrolytes, 3rd ed., Reinhold, New York, 1950.

4. J. H. Hildebrand and R. L. Scott, Regular Solutions, Prentice-Hall, Englewood Cliffs, New Jersey, 1962.

5. C. E. More, Atomic Energy Levels, Vols. I-III, U.S. Govt. Printing Office, Washington 1949, 1952, 1958.

6. Configurations with four to five unpaired d electrons can yield a large number of electronic states corresponding to the various combinations of orbital angular momenta and spin of the electrons. Strictly speaking, one should average the excitation energies of all of the electronic states corresponding to a particular electronic configuration. However, this labor is not necessary for our purpose as the order of the lowest electronic states usually will not differ from the order of the average energies of each configuration by more than 10 kcal/mole which is sufficient accuracy for determining which structures are stable.

7. K. Gschneidner, Jr., Chapter 14 of The Rare Earths, Ed. F. H. Spedding and A. H. Daane, John Wiley, New York, 1961.

8. L. Pauling, Proc. Natl. Acad. Sci., 39, 551 (1953).

9. C. Herring, J. Appl. Phys. Suppl. 31, 3 (1960).

10. R. Kiessling, Met. Rev. 2, 77 (1957).

11. R. Schwarzkopf and R. Kieffer, Refractory Hard Metals, MacMillan, New York, 1953.

12. P. A. Beck, ARL Tech Report 60-326, 1960.

13. A. E. Dwight, Trans. Am. Soc. Metals 53, 479 (1961).

14. M. Hansen and K. Anderko, Constitution of Binary Alloys, McGraw-Hill, New York, 1958.

15. C. E. Lunden, Rare-Earth Phase Diagrams, Chapter 16 of The Rare Earths, Ed. F. H. Spedding and A. H. Daane, John Wiley, New York, 1961.

16. B. T. Matthias, T. H. Geballe, and V. B. Compton, Reviews of Modern Physics, 35, 1 (1963).

17. W. Hume-Rothery, Structures of Metals and Alloys, Institute of Metals, London, 1936.

18. L. Pauling, Proc. Natl. Acad. Sci, 36, 533 (1950).

19. D. I. Bardos, K. P. Gupta, P. A. Beck, Nature 192, 744 (1961).

20. B. N. Das and P. A. Beck, Trans. AIME, 218, 733 (1960) and Trans. AIME, 221, 1687 (1961).

21. W. Bronger and W. Klemm, Z. anorg. allg. Chem., 319, 58 (1962).

22. G. N. Lewis, M. Randall, K. S. Pitzer, and L. Brewer, Thermodynamics, 2nd Ed., McGraw-Hill, New York, 1961.

23. A. Hellawell and W. Hume-Rothery, Phil. Trans. Roy. Soc., Ser A, 249, 417 (1957).

24. W. S. Gibson and W. Hume-Rothery, J. Iron Steel Inst., 189, 243 (1958).

25. A. Hellawell, J. Less-Common Metals, 1, 343 (1959) and 4, 101 (1962).

26. W. Hume-Rothery, Phil Mag., 6, 769 (1961).

27. E. M. Savitskii and C. V. Kopetskii, Z. Neorg. Khim., 5, 2414 (1960).

28. E. M. Savitskii and C. V. Kopetskii, Z. Neorg. Khim., 5, 755 (1960).

29. E. M. Savitskii and C. V. Kopetskii, Z. Neorg. Khim., 5, 2638 (1961).

30. E. M. Savitskii, M. A. Tylkina, R. V. Kirelenko, and C. V. Kopetskii, Z. Neorg. Khim., 6, 1474 (1961).

31. E. D. Eastman, L. Brewer, L. A. Bromley, P. W. Gilles, and N. L. Lofgren, J. Am. Chem. Soc. 72, 2248, 4019 (1950).

32. A. T. Aldred, Trans. AIME, 224, 1082 (1962).

33. A. Dwight, Trans. AIME, 215, 283 (1959).

34. E. Raub, J. Less-Common Metals, 1, 3 (1959).

35. A. A. Rudnitskii and R. S. Polyakov, Z. Neorg. Khim, 4, 1404 (1959).

36. W. Obrowski and G. Zwingsman, Z. Metallkunde, 53, (7), 543 (1962).

37. M. A. Tylkina, I. A. Tsyganov, and E. M. Savitskii, Z. Neorg. Khim., 7, 1917 (1962).

38. A. A. Rudnitskii and N. A. Birun, Z. Neorg. Khim., 5, 2414 (1960).

39. K. Anderko, Z. Metalk., 50, 681 (1959).

40. Y. L. Yao, Trans. Met. Soc. AIME, 224, 1146 (1962).

41. H. J. Wallbaum, Naturw., 31, 91 (1943).

42. A. E. Dwight and P. A. Beck, Trans. Met. Soc. AIME, 215, 976 (1959).

43. W. Hume-Rothery, "The Problem of the Transition Metals," paper in Electronic Structure and Alloy Chemistry of the Transition Elements, p. 83, Ed. by Paul A. Beck, Interscience, 1963.

44. V. M. Nevitt, "Alloy Chemistry of the Transition Elements," paper in Electronic Structure and Alloy Chemistry of the Transition Elements, p. 101, Ed. by Paul A. Beck, Interscience, 1963.

45. F. Laves in Theory of Alloy Phases, Amer, Soc. for Metals, Cleveland, 1956.

46. P. Greenfield and P. A. Beck, Trans. AIME, 206, 265 (1956).

47. K. P. Gupta, N. S. Rajan, and P. A. Beck, Trans. AIME, 218, 617 (1960).

48. J. G. Croeni, C. E. Armantrout, and H. Kato, U.S. Bur.Mines Report of Investigations 6079 (1962).

49. W. B. Pearson and W. Hume-Rothery, J. Inst. Metals, 81, 311 (1952-3).

50. O. K. Kuo, Acta. Met., 1, 301 (1953).

51. H. Nowotny, "Alloy Chemistry of Transition Element Borides, Carbides, Nitrides, Aluminides, and Silicides, "paper in Electronic Structure and Alloy Chemistry of the Transition Elements, p. 179, Ed. by Paul A. Beck, Interscience, 1963.

52. M. V. Nevitt, J. W. Downey, R. A. Morris, Trans.Met. Soc. AIME, 218, 1019 (1961).

53. E. M. Savitskii, M. A. Tylkina, Y. A. Zot'ev, Z. Neorg. Khim, 4, 702 (1956).

54. A. Taylor, N. J. Doyle, B. J. Kagle, J. Less Common Metals, 3, 265 (1961).

55. J. H. Brophy, P. Schwarzkopf, and J. Wulf, Trans. Met. Soc. AIME, 218, 910 (1960).

56. J. B. Darby, Jr., D. J. Lam, L. J. Norton and J. W. Downey, J. Less Common Metals, 4, 558 (1962).

57. G. R. Purdy and J. G. Parr, Trans. Met. Soc. AIME, 221, 636 (1961).

58. C. J. Raub and C. A. Anderson, Bull Am. Phys. Soc., March 1963 Meeting Abstracts.

59. M. E. Kirkpatrick and W. L. Larsen, Trans. ASM, 54, 580 (1961).

60. M. E. Kirkpatrick, J. F. Smith and W. L. Larsen, Acta Cryst., 15, 894 (1962).

61. V. N. Svechnikov and A. T. Spektor, Dokl. Akad. Nauk SSR, 143, 613 (1962).

62. W. L. Larsen, W. H. Pechlin, and D. E. Williams, AEC Report IS-500, pg. M-40 (9/62).

63. R. W. Waterstrat, B. N. Das, P. A. Beck, Trans. Met. Soc. AIME, 224, 512 (1962).

64. R. W. Fountain and W. D. Forgeng, Trans. Met. Soc. AIME, 215, 998 (1959).

65. R. W. Fountain, G. M. Faulring, and W. D. Forgeng, Trans. Met. Soc. AIME, 221, 747 (1961).

66. E. J. Rapperport and M. F. Smith, J. Metals, 13, 86 (1961).

67. N. J. Grant and B. C. Giessen, WADD Tech. Report 60-132, Part II, pg. 147 (1962).

68. B. C. Giessen, R. Nordheim, and N. J. Grant, Trans. Met. Soc. AIME, 221, 1009 (1961).

69. A. G. Knapton, J. Less Common Metals, 2, 113 (1960).

70. W. Rostoker, WADC Tech. Report 59-492, March 1960.

71. N. J. Grant and B. Giessen, reported by E. J. Rapperport, NMI-9246, 9250-9252 (1963).

72. H. Kimura and A. Ito, J. Jap. Inst. Metals, 25, 88 (1961).

73. S. Komjathy, J. Less Common Metals, 3, 486 (1961).

74. M. A. Tylkina, K. V. Povarova, E. M. Savitskii, Proc. Acad. Sci. USSR, 131, 332 (1960); Z. Neorg. Khim 5, 1907 (1960).

75. A. G. Knapton, J. Inst. Metals, 87, 28 (1958).

76. J. Brophy as reported by E. J. Rapperport, NMI-9246 and 9252 (1963).

77. E. M. Savitskii, V. V. Baron, A. N. Khotinskaya, Z. Neorg. Khim, 6, 2603 (1961).

78. E. Raub and W. Fritzsche, Z. Metallk., 54, 21 (1963).

79. W. Koster and W. D. Hahl, Z. Metallk., 49, 647 (1958).

80. J. H. Auld and N. E. Ryan, J. Less Common Metals, 3, 221 (1961).

81. R. D. Dragsdorf and W. D. Forgeng, Acta Cryst., 15, 531 (1962).

82. I. Kornilov and E. N. Pylaeva, Z. Neorg. Khim, 7, 590 (1962).

83. H. J. Goldschmidt and J. A. Brand, J. Less Common Metals, 3, 44 (1961).

84. E. Bucher, F. Heiniger, and J. Muller, Helv. Phys. Acta, 34, 843 (1961).

85. J. H. Brophy, M. H. Kamdar, J. Wulff, Trans. Met. Soc. AIME, 221, 1137 (1961).

86. A. Taylor, B. J. Kagle, and N. J. Doyle, J. Less Common Metals, 3, 333 (1961).

87. E. J. Rapperport and M. F. Smith, WADD Technical Report 60-132 (Part II), (1962).

88. H. Kato and M. I. Copeland, Bur. of Mines BM-U-1031, pg. 19 (1963).

89. L. Northcott, J. Less Common Metals, 3, 125 (1961).

90. A. Taylor, N. J. Doyle, B. J. Kagle, J. Less Common Metals, 4, 436 (1962).

91. B. T. Mathias, T. H. Geballe, V. B. Compton, E. Corenzwit, and G. W. Hull, Phys. Rev., 128, 588 (1962).

92. M. A. Tylkina, V. P. Polyakova, E. M. Savitskii, Z. Neorg. Khim, 6, 1471 (1961).

93. J. B. Darby Jr. and S. T. Zegler, J. Phys. Chem. Solids, 23, 1825 (1962).

94. E. Anderson and W. Hume-Rothery, J. Less Common Metals, 2, 443 (1960).

95. E. Anderson and W. Hume-Rothery, J. Less Common Metals, 2, 19 (1960).

96. C. W. Haworth and W. Hume-Rothery, J. Inst. Metals, 87, 265 (1958-9).

97. E. M. Savitskii, V. F. Terekhova and N. A. Birun, Z. Neorg. Khim, 6, 1960 (1961).

98. E. C. van Reuth, Trans. Met. Soc. AIME, 215, 216 (1959).

99. R. F. Smart and F. G. Haynes, J. Inst. Metals, 91, 153 (1962).

100. D. T. Cromer and A. C. Larson, Acta. Cryst., 12, 855 (1959).

101. R. A. Buckley and W. Hume-Rothery, J. Iron Steel Inst., 201, 121 (1963).

102. N. V. Ageev and V. S. Shekhtman, Proc. Acad. Sci. Chem. Sect., 143, 1091 (1962); Chem. Tech. Sect., 143, 922 (1962).

103. E. Raub and W. Plate, Z. Metallk., 51, 477 (1961).

104. E. Raub and D. Menzel, Z. Metallk, 52, 831 (1961).

105. H. J. Goldschmidt, Research, 10, 289 (1957).

106. B. C. Giessen, I. Rump, N. J. Grant, Trans. Met. Soc. AIME, 224, 60 (1962).

107. A. Taylor, B. J. Kagle, N. J. Doyle, J. Less Common Metals, 5, 26 (1963).

108. E. M. Savitskii and M. A. Tylkina, "Phase Diagrams of Re With Transition Metals," pg. 67, Rhenium, Ed. by B. W. Gonser, Elsevier Publishing Co., N.Y., 1962.

109. S. Saito and P. A. Beck, Trans. Met. Soc. AIME, 218, 680 (1960).

110. R. E. Siebold and L. S. Berks, J. Nucl. Materials, 3, 260 (1961).

111. B. D. Browning, "Platinun Rich Portion of the System Ta-Pt" Technical Report AD-269-414, 1961.

112. H. Braun and K. Sedlatschek in Powder Metallurgy, Ed. W. Leszynski, Interscience, New York, 1961.

113. The internal pressures of the solid metals at room temperature are given in Table 23 in Section VIII of this paper.

114. The tabulation of enthalpies of sublimation of the metals given in reference 2 is reproduced in Table 22of this paper with minor corrections.

115. The tabulation of crystal structures of the elements given in reference 2 is reproduced in Table 24 in Section VIII of this paper with minor additions of newer data as noted in Section IV.

116. R. M. Waterstrat, Trans. Met. Soc. AIME, 224, 240 (1962).

117. K. Schubert, K. Frank, R. Gohle, A. Maldonado, H. G. Meissner A. Raman, and W. Rossteutscher, Naturwissenschaften 50, No. 2, 41 (1963).